

Accelerating 2PC-based ML with Limited Trusted Hardware

Muqsit Nawaz* Aditya Gulati*[†] Kunlong Liu* Vishwajeet Agrawal[‡] Prabhanjan Ananth* Trinabh Gupta*

*UCSB [†]IIT Kanpur [‡]IIT Delhi

Abstract

This paper describes the design, implementation, and evaluation of Otak, a system that allows two non-colluding cloud providers to run machine learning (ML) inference without knowing the inputs to inference. Prior work for this problem mostly relies on advanced cryptography such as two-party secure computation (2PC) protocols that provide rigorous guarantees but suffer from high resource overhead. Otak improves efficiency via a new 2PC protocol that (i) tailors recent primitives such as function and homomorphic secret sharing to ML inference, and (ii) uses trusted hardware in a limited capacity to bootstrap the protocol. At the same time, Otak reduces trust assumptions on trusted hardware by running a small code inside the hardware, restricting its use to a preprocessing step, and distributing trust over heterogeneous trusted hardware platforms from different vendors. An implementation and evaluation of Otak demonstrates that its CPU and network overhead converted to a dollar amount is $5.4\text{--}385\times$ lower than state-of-the-art 2PC-based works. Besides, Otak’s trusted computing base (code inside trusted hardware) is only 1,300 lines of code, which is $14.6\text{--}29.2\times$ lower than the code-size in prior trusted hardware-based works.

1 Introduction

How can a machine learning (ML) system running in the cloud perform inference without getting access to the inputs to inference (model parameters and the data points whose class is being inferred)?

This question is motivated by a fundamental tension between ease-of-use and confidentiality of user data. On the one hand, cloud providers expose easy-to-use ML APIs [4, 47, 77]. A user can call them with model parameters and input data points, and receive inference results while treating ML as a black-box. Furthermore, the user does not have to provision and manage ML systems locally. On the other hand, ML APIs require inputs in plaintext. Thus, a user’s sensitive or proprietary model parameters and data points can be accessed by rogue system administrators at the cloud provider [31, 39, 113], hackers who can get into the cloud provider’s infrastructure [12, 102], and government agencies [3, 46, 75, 76].

Given the wide array of ML applications, the need to balance the benefits and confidentiality-risks of cloud-hosted ML services has received significant attention (§2.4). A long line of work relies on cryptographic techniques [10, 11, 14, 16, 24, 26, 27, 29, 42, 53, 60, 62, 68, 72, 73, 80, 82, 83, 91, 92, 94, 104, 105, 109]. These works provide rigorous guarantees

but incur high resource overhead (CPU consumption, network transfers, etc.). For example, for a single inference over the ResNet-32 model [52], state-of-the-art systems that run over two non-colluding cloud providers [64, 83] make over 6 GB of expensive, wide-area network transfers (§7.4).

In a quest to avoid expensive cryptography, researchers have resorted to using trusted execution environments (TEEs). A TEE consists of a secure container that can execute a program such that an external entity peeking inside the container learns only the input-output behavior of the computation. Secure systems developed using TEEs not only are less complex (and hence, easier to build) but also offer significant efficiency benefits over their counterparts built only using cryptography. Indeed, there are many highly efficient systems developed over the years [38, 54–56, 84, 85, 99, 100]. For instance, the PRIVADO system for ML inference incurs less than 20% overhead relative to a non-private system [99].

However, TEEs are not a panacea for building secure systems. Over the years, researchers have discovered various cryptanalytic attacks. First, the code inside a TEE can leak sensitive data through bugs and digital side-channels [23, 32, 49, 70, 81, 103, 110], although these leaks can be mitigated by making code data-oblivious [56, 85, 89, 99], and formally proving the absence of digital side-channels and bugs [15]. Second, TEEs can leak data through analog side-channels such as power draw, and physical side-channels such as bus tapping [40, 41, 65]. Third, current systems use a single TEE which opens up the possibility that the hardware designer or someone along the supply chain injects a backdoor into the hardware [30, 36, 93, 106]. Thus, current TEE-based systems also rely on the assumption that the TEE vendor is trustworthy.

We introduce Otak, a new two-server ML inference system in the honest-but-curious model. Otak uses cryptography but runs a piece of functionality inside TEEs to remove some weight from cryptography, giving a substantially less expensive system that solely using cryptography. The use of TEEs does create a trusted computing base (TCB), consisting of both the code that runs inside the TEEs, and the hardware design and implementation of the TEE itself. However, Otak lowers the size of the TCB, by (i) reducing the size of the functionality running inside the TEE, (ii) distributing trust over heterogeneous TEEs from different vendors such that the confidentiality of the system is preserved even if a TEE is compromised.

Otak performs (i) and (ii) above for reducing TCB size in two progressive design steps that we call *reducing-TEE-code* and *distributing-trust*.

Techniques for reducing-TEE-code step. Otak starts by observing that ML inference computation for many types of models, particularly, neural networks, can be expressed as a series of layers, where each layer performs either a linear computation (a vector-matrix product) or a non-linear computation (an activation function such as Rectified Linear Unit or ReLU), or both (§2.1). Thus, a secure solution for ML inference requires sub-protocols for linear and non-linear computations.

A common way to perform these computations over two servers is to use the Beaver multiplication protocol to compute vector-matrix products [13] and Yao’s garbled circuit protocol [111] to compute non-linear functions. Further, Beaver’s protocol requires the two servers to hold correlated randomness called Beaver triple shares, which is typically generated using additive homomorphic encryption [64, 83]. A challenge with existing protocols is that both Beaver triple generation and Yao’s protocol incur significant expense. For instance, Yao’s protocol requires transferring a verbose Boolean circuit representation of the non-linear function between the servers.

Otak makes two changes to this protocol. First, instead of using additive homomorphic encryption to generate Beaver triple shares, it uses a new protocol based on homomorphic secret sharing or HSS [18, 21, 22] (§4). This protocol contains a packing technique that optimally uses the input space of HSS operations, thereby reducing overhead relative to additive homomorphic encryption-based solutions. For instance, network overhead in Otak’s protocol for a vector-matrix product over a matrix with 1024×1024 entries is at least $7.6 \times$ lower relative to prior work (§7.2).

Second, Otak replaces Yao’s general-purpose protocol with a recent protocol of Boyle, Gilboa, and Ishai (BGI) [20] that is efficient for computing non-linear functions. This protocol consumes slightly more CPU than Yao, but incurs significantly lower network overhead (for instance, by $460 \times$ for the ReLU function; §7.3).

The BGI protocol is promising; however, applying it to ML inference creates two issues. First, the protocol, as described in the literature can efficiently encode the ReLU function (and approximations of Sigmoid and Tanh) but not the MaxPool and Argmax functions [20, 95] (§3). The core issue is that the BGI protocol depends on the function secret sharing (FSS) primitive [17, 19], whose current constructions exist only for two functions, a point function and an interval functions, that do not naturally encode the max function. The second issue with the BGI protocol is that it assumes that the two servers hold correlated randomness: shares of keys for FSS.

Otak fixes the first issue via new encodings of MaxPool and Argmax atop point and interval functions (§3). These encodings may be of independent interest. Otak fixes the second issue by generating the FSS keys inside a TEE per server. Since all non-linear functions further call just the point and interval functions, the code for FSS key generation is small.

Techniques for distributing-trust step. The protocol so far is efficient but contains TEEs as a single point of attack. In

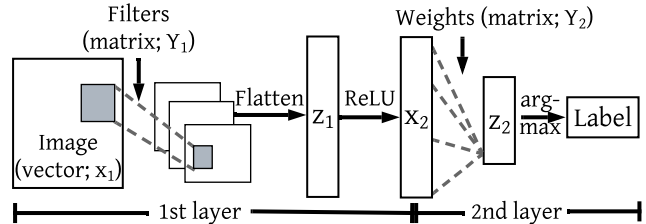


FIGURE 1—An example CNN with two layers. Each layer computes a vector-matrix product (e.g., $z_1 = x_1 \cdot Y_1$) and applies a non-linear function (e.g., ReLU).

the distributing-trust step, Otak takes FSS key generation from inside the TEEs and distributes it over *multiple, heterogeneous* TEEs from different vendors. In particular, Otak replaces one TEE per server with three TEEs per server and runs a three-party secure computation protocol (3PC) over the TEEs such that an adversary does not learn the FSS keys even if it corrupts one of the TEEs.

General-purpose 3PC protocols can be expensive. However, Otak again notes that all ML non-linear functions can be encoded on top of the point and interval functions. So it devises a new customized 3PC protocol for the limited functionality of generating FSS keys for point and interval functions. Otak’s customized protocol is cheaper, for instance, by $30 \times$ in terms of network transfers, relative to a general solution (§5).

Evaluation results. We have implemented (§6) and evaluated (§7) a prototype of Otak. Our prototype runs over two cloud providers, Microsoft Azure and Amazon AWS, with multiple TEE machines per provider. Our prototype demonstrates two properties of Otak. First, its code inside the TEE is 14.6 – $29.2 \times$ smaller relative to existing single TEE-based systems (in absolute terms, it is less than 1,300 lines of code). Second, for several ML models including a 32-layer ResNet-32 [52], and for several datasets including those for speech and image recognition, Otak’s dollar cost to perform inference (that is, CPU and network consumption converted to a dollar amount) is 5.4 – $385 \times$ lower than prior state-of-the-art cryptography-based works that run over two non-colluding servers.

2 Overview of Otak

2.1 Private outsourced ML inference

Otak targets the problem of private outsourced ML inference. This problem revolves around three parties: an *ML model owner*, a *service provider*, and a *data point owner*. The model owner trains a model and deploys it at the service provider, whose task is to label new data points supplied by the data point owner against the model, for example, tell whether an image contains a human or not. The privacy aspect of the problem requires that (a) the service provider must not learn the model parameters or the data points, (b) the model owner must not learn the data points, and (c) the data point owner must learn only the inference result.

While many types of ML models exist, Otak focuses on

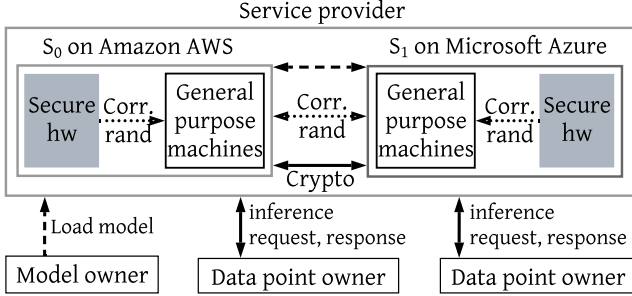


FIGURE 2—Otak’s high-level architecture.

neural networks [44, 51], in particular, feedforward neural networks (FNNs) and convolutional neural networks (CNNs), for two reasons. First, FNNs and CNNs have a wide array of applications, from speech recognition [1], to computer vision [67], to chemical analysis [97]. Second, one can express inference for other models such as support vector machines, Naive Bayes, and regression as inference over FNNs [83].

Fundamentally, FNNs and CNNs rely on slightly different building blocks. For instance, the former employs dense layers while the latter additionally uses convolutions. However, one can abstract inference for both types of models into a common structure. This structure is a series of *layers*, where each layer computes a vector-matrix product and applies a non-linear function such as ReLU (Rectified Linear Unit), Sigmoid, MaxPool, Argmax, and Tanh to the product [44]. Figure 1 illustrates the structure of an example CNN.

2.2 Architecture

Figure 2 shows Otak’s architecture. Otak consists of a service provider, and multiple model and data point owners. The service provider runs two servers, S_0 and S_1 , in separate administrative domains such as Microsoft Azure and Amazon AWS. Each server contains TEE machines from different vendors (labeled collectively as “secure hw” in the figure), and general-purpose compute machines (labeled collectively as “general-purpose machines” in the figure).

At a high level, Otak’s protocol to privately outsource inference has four phases: *setup*, *model-loading*, *preprocessing*, and *online*.

- **Setup:** The setup phase (not depicted in Figure 2) runs once between the Otak’s two servers. During setup, the servers generate long-lived cryptographic material such as seeds for a pseudorandom number generator. This cryptographic material is reused across all inference requests.
- **Model-loading:** This phase (dashed arrows in Fig. 2) runs once per model. In this phase, the model owner uploads *secret-shares* (over a field) of the model parameters to the two servers, who transform and store them. We denote sh_b^{MP} as the share given by model owner to S_b , for $b \in \{0, 1\}$.
- **Preprocessing:** The preprocessing phase runs once per inference, and precedes the online phase. In the preprocessing

phase (depicted by dotted arrows in Figure 2), Otak’s servers generate *correlated randomness* (depicted as “corr rand” in the figure). This correlated randomness does not depend on the values of the model parameters or the data points. This phase uses the TEE machines.

- **Online:** The online phase (depicted by solid arrows in Figure 2) runs once per inference and is input-dependent. In this phase, the data point owner uploads secret-shares (over a field) of its data point to the two servers (we denote the share sh_b^{DP} as the share given to S_b), who run a cryptographic protocol using these shares and the outputs from the other phases, and generate shares of the inference label. Finally, each server sends its share of the label to the data point owner, who combines the shares to get the actual label.

Definition 2.1 (Correctness). For every input $sh_b^{MP} \in \{0, 1\}^{\text{poly}(\lambda)}$, $sh_b^{DP} \in \{0, 1\}^{\text{poly}(\lambda)}$ (corresponding to a data-point DP sent by the data-point owner, and additive secret-shares of model parameters $MP = \{Y_0, Y_1, \dots, Y_{L-1}\}$ for a L -layer model sent by the model-owner) to S_b , the reconstruction of the secret-shares output by both servers S_0, S_1 equals the prediction output of applying the model with parameters MP to input DP .

2.3 Threat model and security definitions

Otak considers an honest-but-curious adversary. This adversary follows the description of the protocol but tries to infer sensitive data by inspecting protocol messages. Below, we formally define Otak’s security notion.

We consider two settings, namely *single-TEE* and *multiple-TEE*, depending on how many TEEs Otak’s servers employ. In the *single-TEE* setting, Otak’s servers use one TEE each.¹ We denote the TEE used by S_b as T_b , for $b \in \{0, 1\}$. Further, we denote the functionality implemented by T_b as \mathcal{F}_b . Finally, we denote non-TEE machines at S_b collectively as M_b . In the *multiple-TEE* setting, each server uses three types of TEEs (made by three different vendors); we denote S_b ’s three types of TEEs by $T_b^{(i)}$ for $i \in \{0, 1, 2\}$ such that i -th TEE $T_b^{(i)}$ implements functionality $\mathcal{F}_b^{(i)}$. We define security for the two settings separately.

Definition 2.2 (Single-TEE security). A single-TEE Otak scheme consisting of setup, model-loading, preprocessing, and online phases is said to be ϵ -secure if for any honest-but-curious (passive) probabilistic polynomial time (PPT) adversary \mathcal{A} corrupting M_b for $b \in \{0, 1\}$ with access to TEE T_b implementing \mathcal{F}_b , for every large enough security parameter λ , there exists a PPT simulator Sim such that the following holds:

for all inputs $sh_b^{MP} \in \{0, 1\}^{\text{poly}(\lambda)}$, $sh_b^{DP} \in \{0, 1\}^{\text{poly}(\lambda)}$ to S_b , randomness $r_b \in \{0, 1\}^{\text{poly}(\lambda)}$,

$$\{\text{View}_{\mathcal{A}}^{\mathcal{F}_b}(1^\lambda, sh_b^{MP}, sh_b^{DP}; r_b)\} \approx_{c, \epsilon}$$

¹The TEE is logically centralized but may be distributed over many physical TEE machines of the same type.

$$\{\text{Sim}(1^\lambda, sh_b^{MP}, sh_b^{DP}, r_b)\}.$$

If ε is negligible in the security parameter, we drop ε in the above definition.

Definition 2.3 (Multiple-TEE security). A multiple-TEE Otak scheme consisting of setup, model-loading, preprocessing, and online phases is said to be ε -secure if, for any honest-but-curious (passive) probabilistic polynomial time (PPT) adversary \mathcal{A} corrupting $M_b, T_b^{(i)}, T_{1-b}^{(i)}$ for $b \in \{0, 1\}, i \in \{0, 1, 2\}$, with access to TEEs $T_b^{(j)}, T_b^{(k)}$ implementing $\mathcal{F}_b^{(j)}, \mathcal{F}_b^{(k)}$ respectively, for $j, k \in \{0, 1, 2\}$ and $j \neq i, k \neq i$, for every large enough security parameter λ , there exists a PPT simulator Sim such that the following holds:

for all inputs $sh_b^{MP} \in \{0, 1\}^{\text{poly}(\lambda)}, sh_b^{DP} \in \{0, 1\}^{\text{poly}(\lambda)}$ to S_b , randomness $r_b \in \{0, 1\}^{\text{poly}(\lambda)}$,

$$\{\text{View}_{\mathcal{A}}^{\mathcal{F}_b^{(j)}, \mathcal{F}_b^{(k)}}(1^\lambda, sh_b^{MP}, sh_b^{DP}; r_b)\} \approx_{c, \varepsilon} \{\text{Sim}(1^\lambda, sh_b^{MP}, sh_b^{DP}, r_b)\}.$$

If ε is negligible in the security parameter, we drop ε in the above definition.

Remark. We assume that TEEs $T_b^{(i)}, T_{1-b}^{(i)}$ come from the same manufacturer.

We do not consider attacks such as membership inference [96] and model stealing [101] that aim to infer membership in training dataset or learn approximate model parameters by observing the black-box behavior of the ML inference system. Although this leakage is an important concern, secure computation alone cannot prevent it. However, defending against such attacks is an active area of research [59, 61, 86]. Besides, these attacks are immaterial when the entity receiving inference outputs also owns the model (that is, when a model owner remotely deploys a model for its own consumption).

2.4 Prior approaches and related work

Several approaches exist in the literature for privately outsourcing the task of inference over FNNs and CNNs. Here, we compare Otak with these prior approaches. While doing the comparison, we include prior works for a restricted setting where the service provider has access to model parameters in plaintext, as the techniques developed for this restricted setting are related to the techniques in Otak’s fully-outsourced setting that also hides model parameters.

One can split prior works into two broad categories: those that rely on TEEs for their security guarantees and those that rely only on cryptography.

TEE-based works. The works based on TEEs use the popular Intel SGX TEE [38, 54–56, 84, 85, 99, 100]. Many of these works [54–56, 85, 99] run a complete ML system inside the TEE. This approach is efficient as the code runs natively on the CPU. However, as indicated earlier (§1), systems based on a single, general-purpose TEE are vulnerable to many attacks.

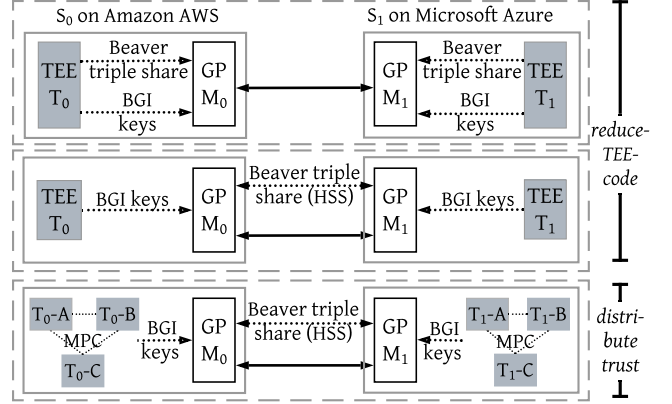


FIGURE 3—Otak’s design steps. Dotted and solid arrows respectively show computation performed during preprocessing and online phases of inference.

Slalom [100], Origami [84], and DFAuth [38] also use Intel SGX, but, like Otak, move parts of inference outside of the TEE. However, these prior systems use the TEE during the online phase of inference, while Otak restricts TEE use to a preprocessing phase. Moreover, Otak removes TEE as a single point of failure by securely distributing trust over heterogeneous TEEs. (Note that, unlike Otak, Slalom and Origami do not hide model parameters from the service provider.)

Cryptography-based works. The alternative approach to using TEEs is to use cryptographic constructs. In particular, a long line of works focuses on building secure ML inference either from secure multiparty computation (MPC) [11, 27, 62, 68, 72, 80, 82, 83, 91, 92, 94, 104, 105], or fully homomorphic encryption (FHE) [10, 14, 16, 24, 26, 29, 42, 53, 60, 73, 95, 109]. However, all these works incur higher overhead in comparison with TEE-based solutions. For instance, a recent state-of-the-art system, Glyph [73], based on FHE, requires 2^n homomorphic operations for a non-linear function over a n -bit input. Otak focuses on the two-server secure computation (2PC) setting; its CPU and network overhead, when converted to dollars, is $5.4\text{--}385\times$ lower than prior 2PC works for this setting (§7.4). One can say that Otak’s use of TEEs helps accelerate cryptography.

2.5 Design approach

As stated in the introduction (§1), Otak adopts the two-step approach of *reducing-TEE-code* and *distributing-trust* for its design. Figure 3 depicts these two steps.

At a high level, Otak starts with a solution that runs ML inference (all four phases) inside a single TEE. It then, gradually, via the *reducing-TEE-code*, moves most of the computation, particularly, the frequently invoked preprocessing and online phases, from inside the TEE to outside the TEE. This step is further divided into two sub-steps: the first sub-step completely gets rid of TEE in the online phase, and the second sub-step splits the preprocessing phase such that the bulk of preprocessing also happens outside the TEE. As a result, Otak

greatly simplifies the computation being performed inside the TEE. Finally, to avoid a single point of attack, Otak employs a secure computation protocol over the computation inside the TEEs to distribute trust among multiple, heterogeneous TEEs.

First part of reducing-TEE-code: online phase without TEE. In this first sub-step of reducing-TEE-code (first row in Figure 3), the TEEs at the two servers run the complete preprocessing phase. In particular, they generate two types of input-independent correlated randomness: *Beaver triple shares* [13] and keys for a cryptographic protocol due to Boyle, Gilboa, and Ishai (BGI) [20]. Meanwhile, the non-TEE machines run the complete online phase (§3).

Second part of reducing-TEE-code: less hardware, more software for the preprocessing phase. In the second sub-step of reducing-TEE-code (illustrated in the middle row in Figure 3), Otak moves a major part of the preprocessing phase—the generation of Beaver triple shares—outside of TEEs. To generate these shares efficiently, the non-TEE machines at Otak’s two servers run an optimized cryptographic protocol based on a recent primitive called homomorphic secret sharing or *HSS* [18, 21, 22] (§4). After the second sub-step of reducing-TEE-code, like a special-purpose cryptoprocessor [9, 57, 58], the TEE machines run the specialized task of generating keys for the BGI protocol.

Distributing-trust. Otak’s distributing-trust step (illustrated in the bottom row in Figure 3) reduces trust on TEEs, by distributing the task of generating keys for BGI onto multiple TEEs. To distribute key-generation efficiently, Otak uses a new, customized three-party secure computation protocol that achieves lower overhead (both CPU consumption and network transfers) than a general-purpose protocol, by shifting the computation of a pseudorandom generator (PRG) (which is the bulk of the computation in the key generation procedure) outside of the general-purpose protocol (§5).

The next three sections (§3, §4, §5) dwell exhaustively on the details of these design steps.

3 Details of first part of reducing-TEE-code

This section describes Otak’s protocol for the first part of its reducing-TEE-code step. To begin with, we focus on one layer of inference, that is, computing one vector-matrix product and applying a non-linear function to the output of the product (§2.1); later in this section, we will relax this assumption.

Figure 4 shows Otak’s protocol for one layer of inference. Say that the vector is $\mathbf{x} \in \mathbb{Z}_p^{1 \times n}$ and the matrix is $\mathbf{Y} \in \mathbb{Z}_p^{n \times m}$, then the protocol computes $f(\mathbf{x} \cdot \mathbf{Y}) \in \mathbb{Z}_p^{1 \times m'}$, where $m' \leq m$, and f is the non-linear function such as ReLU or MaxPool. The vector \mathbf{x} is the data point from the data point owner or the output of the previous layer; the matrix \mathbf{Y} encodes model parameters. All arithmetic is in the field \mathbb{Z}_p for a prime p .

Underneath, the protocol composes Beaver’s secure multiplication protocol [13] with a protocol due to Boyle, Gilboa, and Ishai (BGI) [20]. The Beaver part securely computes the

vector-matrix product: it takes as input the shares of the vector \mathbf{x} and matrix \mathbf{Y} , and the shares of a *Beaver triple* $(\mathbf{a}, \mathbf{B}, \mathbf{c})$, and generates shares of the vector-matrix product $\mathbf{z} = \mathbf{x} \cdot \mathbf{Y}$. For an unfamiliar reader, the Beaver triple $(\mathbf{a}, \mathbf{B}, \mathbf{c})$ is a vector-matrix product over a random vector and matrix. That is, \mathbf{a} and \mathbf{B} are sampled uniformly at random with elements in \mathbb{Z}_p , $\dim(\mathbf{a}) = \dim(\mathbf{x})$, $\dim(\mathbf{B}) = \dim(\mathbf{Y})$, and $\mathbf{c} = \mathbf{a} \cdot \mathbf{B}$.

The BGI part of the protocol computes the non-linear function: it starts with the shares of the vector-matrix product \mathbf{z} , and the shares of the non-linear function f , and computes the shares of the non-linear function applied to the product, that is, shares of $f(\mathbf{z})$. A key enabler of the BGI protocol is the function secret sharing (FSS) primitive (FSS.Gen, FSS.Eval) [17, 19]. FSS.Gen splits a function f into two secret shares f_0 and f_1 , called FSS keys, such that $f_0(x) + f_1(x) = f(x)$. FSS.Eval evaluates a share f_b , for $b \in \{0, 1\}$, on an input x to give a share of $f(x)$ (this happens in step 9 in Figure 4).

The Beaver triples and FSS keys form input-independent correlated randomness. The protocol uses the TEE machines to generate this randomness during the preprocessing phase.

Supporting multiple layers of inference. The protocol above works for one layer of inference. To support multiple layers, Otak replicates the computation inside each phase (except the setup phase) as many times as the number of layers. It then connects copies of the online phase for adjacent layers. Specifically, it feeds the output of step 9, which is a vector in \mathbb{Z}_p , to step 7, which expects a vector of the same type.

Lack of expressibility and fixes. There are two issues with expressibility of the described protocol. First, it assumes arithmetic over the field \mathbb{Z}_p , whereas neural networks perform arithmetic over floating-point numbers. Otak addresses this issue by borrowing standard techniques from the literature to encode floating-point arithmetic as field arithmetic [80, 83]. The conversion results in a drop in inference accuracy; however, this drop is small (§7.4).

The second issue with expressibility is that the BGI part of the protocol can directly handle only certain ML non-linear functions. The restriction is due to the fact that efficient FSS constructions currently exist only for two functions: a point function f_α^β that outputs β at the point α and zero otherwise, and the interval function $f_{(\alpha_1, \alpha_2)}^\beta(x)$ that outputs β if $\alpha_1 \leq x \leq \alpha_2$ and zero otherwise. These functions can express a piece-wise polynomial (that is, a spline) function [20], which in turn can encode the ReLU function and several close approximations [8] of Sigmoid and Tanh. However, a spline cannot directly encode the MaxPool and Argmax functions.

Normally, one would express a max over two values as $\max(x, y) = \text{sign}(x - y) \cdot (x - y) + y$, where the sign function (which is a spline) returns 1 if its input is positive and zero otherwise. However, this formulation of max does not work when the inputs x, y are in \mathbb{Z}_p . For example, consider the case where $x = 5$, $y = 3$, and $p = 7$. For this case, $y > x$ ($x \geq 4$ is considered negative) but $\text{sign}(x - y) = 1$ (+ve). The problem is

Otak’s protocol for first part of its reducing-TEE-code step

- This protocol has two parties, S_0 and S_1 . It computes shares of $f(\mathbf{x} \cdot \mathbf{Y})$, where vector \mathbf{x} is in $\mathbb{Z}_p^{1 \times n}$, matrix \mathbf{Y} is in $\mathbb{Z}_p^{n \times m}$, and f is a non-linear function. We denote $sh_b^{(\mathbf{x})}$ and $sh_b^{(\mathbf{Y})}$ to be S_b ’s shares of \mathbf{x} and \mathbf{Y} respectively.
- The protocol assumes that S_b has a TEE machine T_b and a general-purpose machine M_b . It also assumes several cryptographic primitives, as described below.

Setup phase

1. T_0, T_1 establish a common seed for a pseudorandom function using the Diffie-Hellman protocol [28, 34].

Model-loading phase

2. T_b samples $\mathbf{B} \in_R \mathbb{Z}_p^{n \times m}$ and outputs its share $sh_b^{(\mathbf{B})}$ to M_b .
3. (Receive model parameters \mathbf{Y}) M_0 and M_1 respectively receive $sh_0^{(\mathbf{Y})}$ and $sh_1^{(\mathbf{Y})}$ from the model owner.
4. (Mask \mathbf{Y}) M_0 and M_1 obtain $\mathbf{F} = \mathbf{Y} - \mathbf{B}$, which is a masked version of \mathbf{Y} . To obtain \mathbf{F} , S_b computes $sh_b^{(\mathbf{F})} = sh_b^{(\mathbf{Y})} - sh_b^{(\mathbf{B})}$, sends $sh_b^{(\mathbf{F})}$ to S_{1-b} , receives $sh_{1-b}^{(\mathbf{F})}$ from S_{1-b} , and computes $\mathbf{F} = sh_0^{(\mathbf{F})} + sh_1^{(\mathbf{F})}$.

Preprocessing phase

5. (Generate Beaver triple shares) T_b samples $\mathbf{a} \in_R \mathbb{Z}_p^{1 \times n}$ and computes $\mathbf{c} = \mathbf{a} \cdot \mathbf{B}$. It gives the Beaver triple share $(sh_b^{\mathbf{a}}, sh_b^{\mathbf{B}}, sh_b^{\mathbf{c}})$ to M_b .
6. (Generate FSS keys) T_b samples $\mathbf{r} \in_R \mathbb{Z}_p^{1 \times m}$ and outputs its share $sh_b^{(\mathbf{r})}$ to M_b . T_b also computes FSS keys, k_0 and k_1 , such that $(k_0, k_1) \leftarrow \text{FSS.Gen} \left(1^\lambda, \widehat{f}_{\mathbf{r}} \right)$, where $\widehat{f}_{\mathbf{r}}(\mathbf{in}) = f(\mathbf{in} - \mathbf{r})$ is an offset function for f . T_b outputs key k_b to M_b .

Online phase

7. M_b receives $sh_b^{(\mathbf{x})}$ from the data point owner (or from the output of step 9).
8. (Beaver multiplication) M_b takes matrix \mathbf{F} from the model-loading phase, Beaver triple share $(sh_b^{\mathbf{a}}, sh_b^{\mathbf{B}}, sh_b^{\mathbf{c}})$ from the preprocessing phase, $sh_b^{(\mathbf{x})}$ from the above step, and performs Beaver multiplication [13]. M_b obtains the output $sh_b^{(\mathbf{x} \cdot \mathbf{Y})}$.
9. (BGI evaluation) M_b takes its share of $\mathbf{x} \cdot \mathbf{Y}$ from the above step, and FSS key k_b and randomness $sh_b^{(\mathbf{r})}$ from the preprocessing phase, and outputs $sh_b^{(f(\mathbf{x} \cdot \mathbf{Y}))}$ using the BGI protocol [20].

FIGURE 4—This protocol composes the Beaver multiplication protocol for computing vector-matrix products [13] with the function secret sharing (FSS)-based BGI protocol for computing non-linear functions [20]. The two sub-protocols require correlated randomness, which is generated using TEE machines during the preprocessing phase.

that \mathbb{Z}_p (when it encodes both positive and negative numbers) is not a totally ordered set.

There are many details to how Otak encodes Maxpool and Argmax as a composition of point and interval functions; we leave these details to Appendices A.1 and A.2. However, Otak’s key idea is to split the computation into two parts: when both x and y have the same sign, and when they do not. For the former case, that is, when both x and y are either both positive or both negative, $\text{sign}(x - y)$ gives the right answer. Therefore, one can write $\max(x, y) = \text{ReLU}(x - y) + y$. For the case when x and y have different signs, one can write $\max(x, y) = \text{ReLU}(x) + \text{ReLU}(y)$. Otak composes these two cases, again by using just point and interval functions.

We note that Ryffel et al. in parallel work also encode MaxPool and Argmax using point and interval functions [95]. However, their protocol assumes a trusted third party (besides the two servers). Furthermore, their encoding limits the inputs to a small subset of \mathbb{Z}_p , and incurs network overhead that

is quadratic in the number of input entries to MaxPool and Argmax. In contrast, Otak’s encoding does not have an input restriction, and incurs network overhead linear in the number of input entries to MaxPool and Argmax.

Cost analysis. The cost of setup and model-loading phases in Figure 4 gets amortized across inference requests as model parameters typically change infrequently. Here, we discuss network and CPU costs for the preprocessing and online phases.

Network overhead. In terms of network, the preprocessing phase requires the TEE machines to transfer correlated randomness (Beaver triple shares and FSS keys) to general-purpose machines. These data transfers are within a single administrative domain and cheap. Indeed, popular cloud providers do not charge for intra-domain transfers within a geographical zone [48, 78]. The online phase incurs inter-server (wide-area) network overhead equal to the size of \mathbf{x} plus a small multiple of the size of $\mathbf{z} = \mathbf{x} \cdot \mathbf{Y}$. The first term is due to the Beaver part (step 8 in Figure 4), while the second term

is due to the BGI evaluation part (step 9 in Figure 4). Note that, in contrast, prior work that uses 2PC between two servers (§2.4) uses Yao’s garbled circuits [111] for non-linear functions, whose network overhead is much higher—a multiple of the verbose Boolean circuit representation of the non-linear function. For instance, for ReLU, Otak’s implementation of BGI costs 18 bytes while a recent and optimized implementation of Yao [112] costs 8.3 KB (§7.3).

CPU overhead. In terms of CPU, the Beaver part computes vector-matrix products over small numbers in \mathbb{Z}_p (p is a 52-bit prime in our implementation). Meanwhile, the BGI part runs FSS.Gen and FSS.Eval over the point and interval functions. The CPU for FSS procedures is higher than for Yao (for example, for ReLU, 1.3 ms versus 0.45 ms in Yao; §7.2) as both FSS.Gen and FSS.Eval internally make many calls to AES (for example, FSS.Eval for an interval function over a p -bit input performs $8 \cdot \log p$ AES encryptions). However, since CPU is a much cheaper resource than network consumption, the reduction in network overhead outweighs the increase in CPU.

Security analysis. The protocol described in Figure 4 satisfies the single-TEE security definition in §2.3 (Appendix C.1).

4 Details of second part of reducing-TEE-code

A limitation of the protocol in the previous section is the high amount of computation performed by the TEE machines at the two servers (steps 5 and 6 in Figure 4). In particular, the TEE machines generate FSS keys and Beaver triple shares. Moreover, the latter requires a substantial amount of code inside the TEEs: not only does the TEE compute vector-matrix products but it also runs code to maintain state outside the TEE: for each layer of every model, step 2 in Figure 4 samples and stores a matrix \mathbf{B} , and step 5 reuses this state across inference requests to generate triples. Therefore, Otak’s second part of reducing-TEE-code step moves Beaver triple generation to general-purpose (non-TEE) machines (M_0 and M_1).

Observe that the first two components of a Beaver triple $(\mathbf{a}, \mathbf{B}, \mathbf{c})$ are sampled uniformly at random. Therefore, M_b can locally sample its shares $sh_b^{(\mathbf{a})}$ and $sh_b^{(\mathbf{B})}$ as the sums $\mathbf{a} = sh_0^{(\mathbf{a})} + sh_1^{(\mathbf{a})} \pmod{p}$ and $\mathbf{B} = sh_0^{(\mathbf{B})} + sh_1^{(\mathbf{B})} \pmod{p}$ are also uniformly random. To obtain shares of $\mathbf{c} = \mathbf{a} \cdot \mathbf{B}$ from shares of \mathbf{a} and \mathbf{B} , prior work offers several two-server protocols [62–64, 80, 83]. However, these protocols incur a high inter-server (wide-area) network overhead. For instance, for a vector with 128 entries and a matrix with 128×128 entries, the network overhead of an additive homomorphic encryption-based protocol used in the state-of-the-art prior works [62, 64, 80] is over 1,000 times the size of the vector.

Instead of using prior homomorphic encryption-based protocols, Otak uses a new protocol based on a primitive called homomorphic secret sharing (HSS) that has received much attention recently [18, 21, 22, 37]. Otak’s HSS-based protocol significantly reduces (amortized) network overhead—for instance, to $16\times$ the size of the vector for the specific example above. However, obtaining this performance requires

addressing two challenges of applying HSS to Beaver triple generation. This section gives a necessary background on HSS, explains the challenges, and describes Otak’s protocol.

4.1 Overview of Homomorphic secret sharing (HSS)

Homomorphic secret sharing or HSS [18, 21, 22] is a cryptographic primitive that allows a client to outsource the computation of a program (containing addition and multiplication instructions) to two non-colluding servers such that each server produces its share of the program output without learning the original program inputs.

An HSS scheme has three procedures: HSS.Gen, HSS.Enc, and HSS.Eval. To outsource a program $z = I(x, y, \dots)$ over an input space \mathcal{I} , a client first invokes HSS.Gen to generate HSS keys. These keys consist of a public key, pk , for an underlying encryption scheme, and the shares of the corresponding secret key, $(e_0 = sh_0^{(s)}, e_1 = sh_1^{(s)})$. The client uses the public key to run HSS.Enc and produce a set of ciphertexts, \mathbf{C} , containing encryptions of the program inputs (x, y, \dots) . The client also produces two sets, $\mathbf{S}_0 = \{sh_0^{(x,s)}, sh_0^{(y,s)}, \dots\}$ and $\mathbf{S}_1 = \{sh_1^{(x,s)}, sh_1^{(y,s)}, \dots\}$, containing shares of the program inputs times the secret key. The client sends $(pk, e_0, \mathbf{C}, \mathbf{S}_0)$ to server S_0 , and $(pk, e_1, \mathbf{C}, \mathbf{S}_1)$ to server S_1 . Finally, server S_b locally (without interaction with S_{1-b}) runs HSS.Eval($e_b, \mathbf{C}, \mathbf{S}_b, I$) and gets its share of the program output z .

Otak builds on BKS-LPR = (BKS-LPR.Gen, BKS-LPR.Enc, BKS-LPR.Eval) [22] HSS scheme as it is the most efficient HSS scheme in the literature. There are three notable aspects of BKS-LPR. First, the input space \mathcal{I} is the polynomial ring $R_p = \mathbb{Z}_p[x]/(x^N + 1)$ consisting of all degree $N - 1$ polynomials with coefficients in \mathbb{Z}_p . Second, the underlying encryption scheme that BKS-LPR uses is the LPR scheme [74] with plaintext space R_p . Third, a key instruction that BKS-LPR.Eval supports is *Mult*. This instruction takes as inputs a LPR ciphertext C^x for $x \in R_p$, and a share of an input $y \in R_p$ times the LPR secret key, that is, a share of $y \cdot s$, and outputs a share of the product $x \cdot y$. That is, $sh_b^{(x \cdot y)} \leftarrow \text{Mult}(sh_b^{(y \cdot s)}, C^x)$.

4.2 Promise and perils of BKS-LPR HSS

A key property of BKS-LPR is that it allows a client to outsource computation to two servers that do not interact with each other. However, as described, BKS-LPR is not suitable for Beaver triple generation, for two reasons. First, BKS-LPR requires three parties where one of them supplies BKS-LPR keys and encodings (encryptions and shares) of program inputs. However, in Otak’s setup, there are only two parties—machines M_0 and M_1 . They have shares of a vector \mathbf{a} and a matrix \mathbf{B} , and require shares of $\mathbf{c} = \mathbf{a} \cdot \mathbf{B}$. Therefore, how should M_0, M_1 obtain (i) BKS-LPR keys, (ii) ciphertexts for input \mathbf{a} , and (iii) shares of $\mathbf{B} \cdot s$?

Second, the dimension N of the input space R_p is large, for example, 2^{12} or 2^{13} , to ensure the security of LPR ciphertexts [2, 74]. But oftentimes the vector length in ML models, denoted by n , is smaller than N . For instance, a CNN for the

Otak's protocol after its reducing-TEE-code step

- This protocol assumes the same parties and performs the same computation as the protocol in Figure 4.

Setup phase

- M_0 and M_1 use Yao's garbled circuit protocol [111] to run $(pk, s) \leftarrow \text{BKS-LPR.Gen}(1^\lambda)$. Yao's protocol outputs $(pk, e_b = sh_b^{(s)})$ to M_b . Here, s is a secret key for the LPR encryption scheme.
- The other step of setup is step 1 from Figure 4.

Model-loading phase

- M_b samples $sh_b^{(\mathbf{B})} \in_R \mathbb{Z}_p^{n \times m}$.
- M_0 and M_1 use Yao's protocol to convert shares of each column of \mathbf{B} , that is, $sh_b^{(\mathbf{B}[i])}$ for $i \in \{1, \dots, m\}$, to $sh_b^{(\mathbf{B}[i] \cdot s)}$, where $B[i] \in R_p$ is the polynomial encoding of the column vector $\mathbf{B}[i]$. The polynomial encoding is standard and based on an application of Chinese remainder theorem (CRT) to ring R_p [22].
- Other steps of model-loading are steps 3 and 4 from Figure 4.

Preprocessing phase

- (Generate Beaver triple shares) M_b does the following.
 - Samples $sh_b^{(\mathbf{a})} \in_R \mathbb{Z}_p^{1 \times n}$ and converts it to its polynomial form $sh_b^{(a)}$.
 - (Encrypts a) Sends $C^{sh_b^{(a)}} \leftarrow \text{LPR.Enc}(pk, sh_b^{(a)})$ to M_{1-b} , receives $C^{sh_{1-b}^{(a)}}$ from M_{1-b} , and computes $C^a = C^{sh_b^{(a)}} + C^{sh_{1-b}^{(a)}}$ using the additively homomorphic property of LPR.
 - (Multiplies a with $B[i]$) For each $i \in \{1, \dots, m\}$, computes $sh_b^{(\mathbf{B}[i] \cdot a)} = \text{Mult}(sh_b^{(\mathbf{B}[i] \cdot s)}, C^a)$ using the HSS multiplication instruction. M_b then converts $sh_b^{(\mathbf{B}[i] \cdot a)}$ to its vector form $sh_b^{(\mathbf{B}[i] \odot \mathbf{a})}$, where \odot denotes component-wise multiplication. M_b computes $sh_b^{(\mathbf{c}[i])} = \sum_{j=1}^m sh_b^{(\mathbf{B}[j] \odot \mathbf{a})}[j]$.
- Finally, perform Step 6 from Figure 4.

Online phase is as in Figure 4

FIGURE 5—Otak's protocol after its reducing-TEE-code design step. This protocol does not show the packing optimization, which is illustrated separately in Figure 6.

MNIST dataset [69] has vectors with 128 entries [72]. When $n < N$, a mapping of vectors or matrix rows (of a Beaver triple) to degree $N - 1$ polynomials in R_p wastes space and incurs unnecessary CPU and network overhead (relative to a mapping that would not waste space in the polynomial).²

4.3 Otak's protocol that incorporates BKS-LPR HSS

Figure 5 shows Otak's protocol for the second part of its reducing-TEE-code step. This protocol incorporates BKS-LPR to generate Beaver triple shares, while addressing the aforementioned issues, as follows.

First, the protocol adapts BKS-LPR for two parties by using the general-purpose Yao's garbled circuit protocol [111] to simulate the client's role. Yao's protocol generates BKS-LPR keys (step 1 under setup in Figure 5) and shares of $\mathbf{B} \cdot s$ to supply to the BKS-LPR Mult instruction (step 4 under model-loading in Figure 5).

Second, the protocol allows M_0 and M_1 to generate LPR ciphertexts for \mathbf{a} using the additively homomorphic properties of LPR. In particular, M_0 and M_1 generate ciphertexts for shares of \mathbf{a} , exchange them, and add them to get a ciphertext

²When $n > N$, the vector-matrix product is split into smaller products akin to block-matrix multiplication. In this case, the last product has a vector of size $n - \lfloor n/N \rfloor \cdot N$, which is $\leq N$.

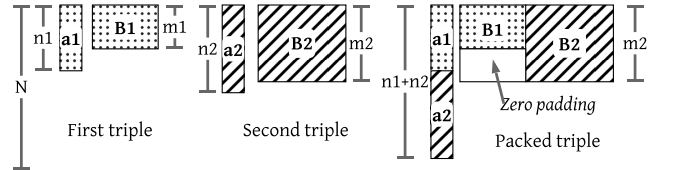


FIGURE 6—Packing scheme for triple generation.

for \mathbf{a} (step 6b in Figure 5). With this change and the one above, the first challenge of applying BKS-LPR to Beaver triple generation is addressed.

Third, the protocol addresses the inefficiency caused by mapping small vectors in \mathbb{Z}_p^n to degree $N - 1$ polynomials in R_p by *packing* multiple smaller triples into an N -sized triple. Figure 6 depicts the overall idea. Say that Otak needs to generate two triples $(\mathbf{a}_1, \mathbf{B}_1, \mathbf{c}_1)$ and $(\mathbf{a}_2, \mathbf{B}_2, \mathbf{c}_2)$ for different layers of the same model, or different layers across models, or different requests to the same layer of a model. Then, instead of running triple generation (step 6 in Figure 5) separately for the two triples, Otak runs a single instance of triple generation.

Cost analysis. Relative to the protocol in Figure 4, the cost of the setup and model-loading phases increases because of the addition of Yao's protocol. However, Yao is used only during setup and model-loading phases, and thus its cost gets

amortized across many inference requests, as setup runs once and model-loading runs once per model.

The preprocessing phase adds inter-server network overhead to generate ciphertexts for \mathbf{a} (step 6b in Figure 5); this overhead is a small multiple of \mathbf{a} 's size due to the packing technique. The preprocessing phase adds CPU cost, mainly due to the calls to LPR encryption function and the HSS Mult instruction. (The online phase does not change relative to Figure 4, so its costs do not get affected.)

Security analysis. The protocol's security follows from the security of BKS-LPR and Yao's garbled circuits. In particular, the protocol satisfies the single-TEE definition in §2.3. Appendix C.1 contains the proof.

5 Details of distributing-trust step

The protocol has so far assumed a single TEE per server. In particular,

- (i) step 1 in Figure 4 uses the TEE T_b at server S_b to set up a common seed for a PRF so that the TEEs at the two servers generate the same sequence of random values,
- (ii) step 6 in Figure 4 uses the TEE machine T_b at server S_b to sample randomness \mathbf{r} and output sh_b^r to M_b , and
- (iii) the same step uses the TEE machine T_b to run $(k_0, k_1) \leftarrow \text{FSS.Gen}(1^\lambda, \hat{f}_r)$ and output FSS key k_b to M_b .

In this section, we remove the single TEE limitation, by distributing the computation in these steps over multiple, heterogeneous TEE machines.

First off, in the multiple-TEE setting, both servers S_0, S_1 consist of a group of three TEEs denoted by $T_0^{(0)}, T_0^{(1)}, T_0^{(2)}$ and $T_1^{(0)}, T_1^{(1)}, T_1^{(2)}$ respectively.

Then, to distribute the first part above (under bullet (i)), each pair of TEEs $(T_0^{(i)}, T_1^{(i)})$ for $i \in \{0, 1, 2\}$ establishes a common PRF seed, say $seed_i$, using the Diffie-Hellman key exchange protocol [28, 34]. A common PRF seed ensures that both TEE machines in a pair (where one comes from either server) generate the same sequence of random values.

Next, to distribute the second part above (generation of \mathbf{r} under bullet (ii) above), each TEE samples randomness locally and considers it to be its share of \mathbf{r} . In more detail, let r be a component of the randomness vector \mathbf{r} , and r_0, r_1, r_2 be uniformly random elements in \mathbb{Z}_p such that $r_0 + r_1 + r_2 = r \pmod{p}$. Then, each TEE $T_b^{(i)}$ for $i \in \{0, 1, 2\}$ executes the procedure GenRand in Figure 4 to sample r_i . Further, TEE $T_b^{(i)}$ sends a share of r_i , that is, $sh_b^{r_i}$, to M_b . Machine M_b receives shares $sh_b^{r_0}, sh_b^{r_1}$, and $sh_b^{r_2}$ from $T_b^{(0)}, T_b^{(1)}$, and $T_b^{(2)}$ respectively, and computes $sh_b^r = sh_b^{r_0} + sh_b^{r_1} + sh_b^{r_2}$.

Finally, to distribute the third part (FSS key generation under bullet (iii) above), a natural starting point is to use a general-purpose three-party MPC protocol [43, 111]. However, general-purpose protocols are expensive. Instead, Otak observes that the task at hand is to compute FSS keys for only

GenRand ($b, seed_i$):

```

 $r_i \leftarrow \text{PRF}_{seed_i}(counter) \pmod{p}$ 
 $sh_0^{r_i} \leftarrow \text{PRF}_{seed_i}(counter + 1) \pmod{p}$ 
 $sh_1^{r_i} \leftarrow r_i - sh_0^{r_i} \pmod{p}$ 
return  $sh_b^{r_i}$ 

```

FIGURE 7—Procedure that TEE $T_b^{(i)}$ runs to distributively generate randomness needed for the BGI protocol (\mathbf{r} in step 6 in Figure 4).

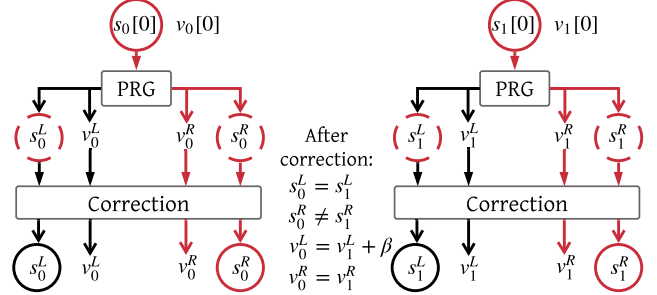


FIGURE 8—Pictorial depiction of the underlying computation in FSS.Gen [17, 19]. The procedure expands two paths in a binary tree; for each node in the path, it invokes a PRG.

the point and interval functions as they can express all common non-linear functions (§3). Thus, Otak uses a customized protocol for the point and interval functions, thereby reducing overhead in comparison to a general solution. In the rest of this section, we focus on this protocol; we first give a brief overview of FSS.Gen and then describe the protocol.

Overview of FSS.Gen. The FSS scheme of Boyle et al. is sophisticated [17, 19]. Moreover, one does not need to understand its low-level details to understand Otak's protocol. For these reasons, we describe only the notable aspects of Boyle et al.'s scheme.

Figure 8 shows the key idea behind FSS.Gen. Essentially, the keys k_0, k_1 output by FSS.Gen are paths from root to leaf nodes in two correlated trees. At each step of path traversal, FSS.Gen takes a random string and performs two computations: (i) expands the random string to two random strings for the two children, and (ii) corrects the value of the children's strings so that they satisfy a certain constraint. These two computations are depicted in Figure 8 as the "PRG" (pseudorandom number generator) and "correction" blocks. The former is usually instantiated using AES and incurs significant expense when performed inside MPC (we use ABY³ [82] in our implementation; §6). Meanwhile, the correction step is cheap as it mainly consists of XORs, which are typically efficient in MPC. Therefore, Otak's goal is to reduce the cost of invoking the PRG.

Otak's protocol for FSS.Gen. Otak's idea is to bring the invocation of the PRG "outside" of the general-purpose MPC protocol. Suppose that when the three TEE machines at server S_b , that is, $T_b^{(0)}, T_b^{(1)}, T_b^{(2)}$, reach the PRG step, they hold XOR-shares of a string $x \in \{0, 1\}^\lambda$ that they have to expand by ap-

plying a PRG, G . That is, $T_b^{(j)}$ holds x_j such that $x_0 \oplus x_1 \oplus x_2 = x$. Then, to obtain strings that are computationally indistinguishable from the shares of $G(x)$, $T_b^{(j)}$ does the following:

- Splits x_j into three blocks $x_j = x_j[0] || x_j[1] || x_j[2]$, where $||$ denotes string concatenation.
- Sends $x_j[i]$ and $x_j[k]$ (for $i, k \in \{0, 1, 2\}$ such that $i \neq j, k \neq j$) to $T_b^{(i)}, T_b^{(k)}$, respectively. After this step, $T_b^{(0)}, T_b^{(1)}$, and $T_b^{(2)}$, obtain $x[0], x[1]$, and $x[2]$, respectively. That is, the TEE machines obtain blocks of x from their shares of x .
- Invokes a PRG locally, say g , over $x[j]$ to expand it to the same length as the output of $G(x)$.
- Treats the output of g as its XOR-share of $G(x)$, and continues onto the next step in FSS.Gen.

Security and cost analysis. Appendix B.1 proves that the output of $g(x[j])$ is indistinguishable from a share of $G(x)$ even if two blocks of the seed x of G are revealed to a distinguisher. Further, Appendix C.2 proves that Otak’s protocol with multiple TEEs meets the multiple-TEE security definition in §2.3. Meanwhile, the benefit of the PRG optimization is a reduction in both CPU and network overhead relative to a general MPC solution, as each TEE invokes a PRG natively on its CPU, rather than inside the MPC framework. For instance, the network transfers between the TEE machines reduce from 1.6 MB in ABY³ [82] to 60 KB with the optimization (§7.1).

6 Implementation

We have implemented a prototype of Otak (§2.2, §3–§5). Our prototype builds on existing libraries. It implements the FSS primitives and the BGI protocol (§3) using the libFSS library [107]. It implements the BKS-LPR HSS scheme and our extensions to the scheme (§4) on top of Microsoft’s SEAL library [90]. We borrow small pieces of code from ABY³ [82] and OpenSSL to implement the secure computation protocol for FSS.Gen (§5) atop the Asylo framework [45] for Intel SGX. Finally, Otak’s various components (§2.2) communicate over the gRPC RPC framework [50]. In total, Otak’s prototype adds 17,000 lines of C++ on top of existing libraries; this number is measured using the sloccount Linux utility [108].

7 Evaluation

Our evaluation answers the following questions:

1. What are Otak’s overheads for computing vector-matrix products, ML non-linear functions, and performing inference over popular ML models?
2. How do Otak’s overheads compare to those of the state-of-the-art cryptography-based works?
3. How accurately can Otak perform inference?
4. How big is Otak’s software TCB and how does its size compare to the TCB of systems that run ML inference completely inside TEEs?

vendor	type	vCPUs	RAM (GB)	network (Gbps)	processor	loc.
AWS	m5.4xlarge	16	64	10	Xeon	CA
Azure	D16s-v3	16	64	8	Xeon	CA
Azure	L8s-v2	8	64	3.2	AMD EPYC	WA
Azure	DC1s-v2	1	4	2	Xeon-SGX	VA

FIGURE 9—Machines used in our experiments.

CPU time				
	VecToPoly	PolyToVec	LPR.Enc	HSS.Mult
for HSS	185.0 μ s	168.4 μ s	4.9 ms	3.6 ms

CPU time		network transfers	
for FSS	<i>Single TEE</i>	<i>Multiple TEEs</i>	
Gen (pt. fn.)	47.2 μ s	0.33 ms	43.8 KB
Eval (pt. fn.)	22.1 μ s	147.5 μ s	N/A
Gen (int. fn.)	63.7 μ s	0.44 ms	55.7 KB
Eval (int. fn.)	28.8 μ s	169.3 μ s	N/A

FIGURE 10—CPU times and network transfers for HSS, FSS procedures, averaged over 1000 runs. Standard deviations (not shown) are within 1% percent of the means. Network transfers are intra-domain.

A summary of our evaluation results is as follows:

- Otak’s CPU and network overhead for computing a vector-matrix product is at least 1.5–2.2 \times and 1–60 \times lower depending on vector-matrix dimensions in comparison to state-of-the-art cryptography-based works (§7.2).
- Otak’s CPU overhead is 11.6–45.1 \times higher for computing a non-linear function depending on the function in comparison to the popular Yao method in prior work. However, Otak’s network overhead is 121.9–2819 \times lower (§7.3).
- Otak’s CPU overhead for private inference is higher than prior state-of-the-work cryptography-based work by at most 14.2 \times , while its inter-server network overhead is 46.4–1448 \times lower depending on the ML model (§7.4).
- Given that CPU is cheaper than network resource, Otak’s dollar cost for ML inference is 5.4–385 \times lower than prior work depending on the ML model (§7.4).
- Otak’s inference accuracy is 1–2% lower than TensorFlow’s as it represents floating-point as fixed-point numbers (§7.4).
- Otak runs 1,300 lines of code inside its TEEs, which is 14.6–29.2 \times lower than the amount of code run inside TEEs by prior TEE-based works (§7.5).

Method and setup. We compare Otak’s two variants with single and multiple TEEs per server, which we call Otak-STEE and Otak-MTEE, to several state-of-the-art baseline systems. For the performance-related questions, we compare Otak’s variants to the following cryptography-based systems.

- SecureML [83] and SPDZ [27, 33, 64] are the state-of-the-art systems for the Otak-like setting where inference runs over two non-colluding servers that hold secret shares of model parameters and data points. We run the code of these systems while configuring them to provide honest-but-curious security.

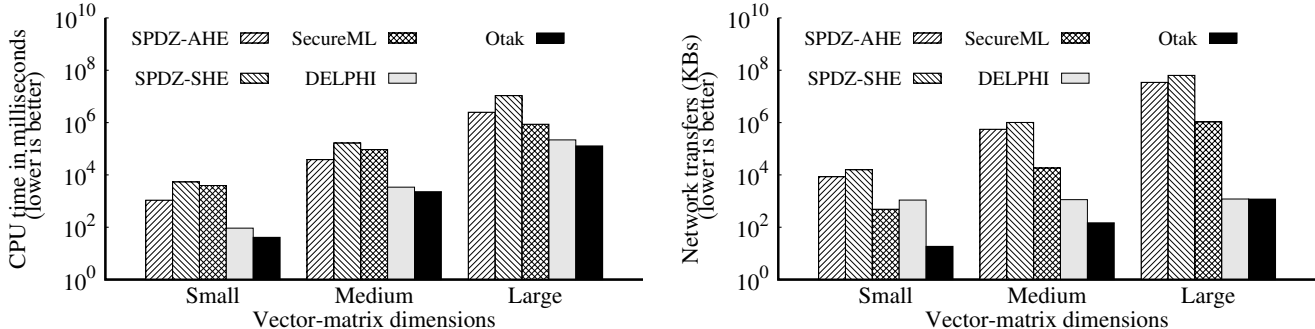


FIGURE 11—CPU times and network transfers for Otak and the baseline systems for privately computing vector-matrix products.

- DELPHI [80] (which optimizes Gazelle [62]) is a recent optimized 2PC system that runs inference between a client (that owns data points) and a server (that owns model parameters). We run DELPHI as a two-server system where one server owns model parameters and the other owns data points. Note that Otak’s comparison to DELPHI is not apples-to-apples as Otak further secret shares model parameters and data points between the two servers so that neither learns them. However, we include DELPHI as it is a recent optimized 2PC system.

For the TCB related questions, we compare Otak to two SGX-based systems: TF Trusted and PRIVADO. TF Trusted is optimized to run TensorFlow Lite inside an Intel SGX TEE [25], while PRIVADO runs a reduced Torch ML framework inside SGX [99]. We pick these two systems from the set of SGX-based systems as their TCBs are either reported or can be measured from their publicly available code.

We run a series of experiments to answer the evaluation questions above. Our experiments deploy a system and vary parameters such as vector-matrix dimensions, the non-linear function (ReLU, Maxpool, Sigmoid, Tanh, Argmax), and the ML model. For the latter, we use four datasets (MNIST [69], CIFAR-10 [66], CIFAR-100 [66], and ISO-LET [35]) and five ML model architectures (two FNNs and three CNNs) including the 32-layer ResNet-32 CNN [52] (Appendix D gives more details). These datasets and models perform a variety of inference tasks including image classification and speech recognition. Our experiments measure inference accuracy for these models as well as resource consumption: CPU time using `std::clock()`, real time (latency) using `std::chrono::high_resolution_clock`, and network transfers using Linux kernel’s `/proc/net/dev`.

Our testbed (Figure 9) is a set of machines on Amazon EC2 and Microsoft Azure. Within these cloud providers, we use both general-purpose and TEE machines. Cloud providers currently offer only Intel SGX-based TEEs [88]; we use two such machines and a regular AMD machine as Otak-MTEE’s three TEEs. In a real deployment, Otak-MTEE would use three different TEEs.

7.1 Microbenchmarks

We begin by presenting CPU and network transfers for primitive operations in Otak’s cryptographic protocols (§3, §4, §5). Figure 10 shows these microbenchmarks.

For computing vector-matrix products, Otak generates Beaver triple shares using the BKS-LPR scheme (§4.3). The first part of the microbenchmarks figure shows the CPU times for BKS-LPR operations: converting a vector to its polynomial encoding and back (used in step 4 and step 6c in Figure 5), generating LPR ciphertexts (step 6b in Figure 5), and performing BKS-LPR multiplication (step 6c in Figure 5). These microbenchmarks are over an `m5.4xlarge` EC2 instance (Figure 9). Note that we configure BKS-LPR for polynomials with $N = 8,192$ coefficients, where each coefficient is up to 52-bits. These parameters are chosen according to the homomorphic encryption standard for a 128-bit security [2].

For computing non-linear functions such as ReLU, Otak relies on the FSS scheme that supports point and interval functions (§3, §5). The second part of the microbenchmarks figure shows CPU times and network transfers (between TEE machines) for FSS procedures (FSS.Gen, FSS.Eval) for the two functions.

7.2 Overheads of computing vector-matrix products

Figure 11 shows the CPU times and (wide-area) network transfers of various systems for computing vector-matrix products while varying the dimensions of the vector and the matrix. The “small”, “medium”, and “large” dimensions correspond to matrices with 128×128 , 1024×1024 , 8192×8192 entries.

CPU overhead. For a particular matrix dimension, Otak (whose two variants do not differ in how they compute vector-matrix products), consumes a lower amount of CPU than SecureML, SPDZ (its both variants based on additive and somewhat homomorphic encryption), and DELPHI. For instance, Otak’s CPU consumption is $6.7\text{--}98.2\times$ lower than SecureML’s, and $1.5\text{--}2.2\times$ lower than DELPHI’s. SecureML consumes a high amount of CPU because it uses the expensive number-theoretic Paillier additive homomorphic encryption scheme [87]. SPDZ and DELPHI use modern additively homomorphic encryption schemes along-with packing techniques [62]. Meanwhile, Otak improves over these works by

	CPU	network (local)	network (wide-area)
ReLU			
Yao	0.45 ms	0	8.3 KB
Otak-STEE	1.3 ms	13.9 KB	18.0 B
Otak-MTEE	5.8 ms	336.8 KB	18.0 B
Sigmoid			
Yao	1.3 ms	0	46.8 KB
Otak-STEE	3.4 ms	37.7 KB	17.0 B
Otak-MTEE	18.5 ms	989.1 KB	17.0 B
Tanh			
Yao	1.44 ms	0	48.6 KB
Otak-STEE	3.3 ms	37.8 KB	18.0 B
Otak-MTEE	16.7 ms	989.9 KB	18.0 B
MaxPool			
Yao	0.45 ms	0	12.2 KB
Otak-STEE	2.9 ms	23.5 KB	89.0 B
Otak-MTEE	20.3 ms	1.2 MB	89.0 B
Argmax			
Yao	0.48 ms	0	12.5 KB
Otak-STEE	3.2 ms	24.8 KB	105.0 B
Otak-MTEE	21.6 ms	1.3 MB	105.0 B

FIGURE 12—CPU times and network transfers for computing non-linear functions using Yao and Otak. The overheads of MaxPool and Argmax depend linearly on the number of input entries; here, we show overhead per entry.

using HSS which enables even more efficient packing for Beaver triple generation (§4.3).

Network overhead. Like for CPU, Otak’s network transfers are lower than those in prior works. For instance, Otak’s overhead is 1–60× lower than DELPHI’s. This is because DELPHI does not optimally use the domain of its underlying encryption scheme; Otak, instead, optimizes the input domain of HSS instructions (§4.3). Note that for “large” matrix dimensions when the size of the vectors equals the dimension of the underlying polynomial ring (8,192), Otak’s overhead is same as DELPHI’s as packing does not take effect. However, for other dimensions, Otak’s packing helps reduce overhead.

7.3 Overheads of computing non-linear functions

Figure 12 shows the overheads of privately computing ReLU, Maxpool, Sigmoid, Tanh, and Argmax using Otak’s FSS-based protocol (§3, §5) and Yao’s garbled circuits—the protocol commonly used in prior two-party systems.

At a high level, Yao’s protocol incurs lower CPU consumption than Otak, especially when Otak uses multiple TEEs. The reason is that the FSS.Eval procedure is more expensive than the evaluation procedure of a Yao’s garbled circuit. Besides, the use of MPC to generate FSS keys adds CPU expense for the multiple TEE case. On the other hand, Yao incurs high wide-area network transfers as it exchanges a large Boolean circuit representing of the non-linear function between the two servers. In contrast, Otak’s wide-area network transfers are small (for example, by a factor of 461× for ReLU) due to the network-efficient online phase of Otak’s FSS-based BGI pro-

ocol (step 9 in Figure 4). Otak does incur intra-domain (local) transfers between TEE machines and between TEE machines and general-purpose machines (step 6 in Figure 4). However, local transfers are cheap. Indeed, popular cloud providers do not charge for intra-domain network transfers within a geographical zone [48, 78]. Overall, the reduction in expensive wide-area network overhead outweighs the increase in cheaper CPU and local network transfers.

The CPU and network costs for Otak follow from microbenchmarks (Figure 10). For instance, ReLU calls the interval function six times. According to Figure 10, six calls to the interval function with multiple TEEs incurs 334.2 KB in local transfers, which is roughly what Figure 12 reports.

7.4 Overheads of private inference

CPU and network overhead. Figure 13 shows CPU and (wide-area) network use for the various systems and ML models.

Otak’s CPU time is higher than the CPU time in prior work. The reason is that Otak requires more CPU for non-linear functions (§7.3), especially when it uses multiple TEEs. However, Otak reduces network transfers (§7.2, §7.3) significantly relative to prior work. For instance, for the ResNet-32 CNN model over the CIFAR-100 dataset (cluster labeled C100-R32 in Figure 13), Otak’s both variants incur 60 MB of wide-area network transfers whereas DELPHI consumes 6 GB, SPDZ with additive homomorphic encryption (SPDZ-AHE) consumes 53.3 GB, and SPDZ with somewhat homomorphic encryption consumes 96.4 GB. Note that SecureML (which we do not show in the figure) currently only implements the ReLU function, so it can encode just the MNIST-FNN (M-FNN) model. For this model, its CPU and network overhead is 9.8× and 46.4×, respectively, higher than Otak’s.

Dollar costs. Otak’s CPU use is higher than prior work while network use is lower. To compare the systems using a common metric, we convert their resource use to a dollar amount.

Figure 14 shows estimated dollar costs for private inference for the various systems. To do the conversion from resource overhead to dollars, we use a pricing model derived from the machine and bandwidth prices of Azure and AWS (Appendix E). This pricing model charges \$0.015–\$0.079 for one hour of CPU time depending on machine type (SGX versus non-SGX), \$0.05 for one GB of outbound network traffic, and zero for local network transfers. The figure shows that Otak’s dollar cost, depending on Otak’s variant, is 9.6–24× lower than SecureML’s, 87–4360× lower than SPDZ’s, and 5.4–55.6× lower than DELPHI’s.

Inference latency. Figure 15 shows the latency of performing inference for the various systems (SecureML is not depicted in the figure, and its latency for M-FNN is 150.2 ms). Overall, Otak takes less time than SecureML (by 2.45×) and SPDZ (by 2.62–262×), but longer than DELPHI (by up to 10.2×) to perform inference. The difference to DELPHI is fundamental—DELPHI targets a non-outsourced setting where model parameters are in plaintext while Otak hides the model parameters

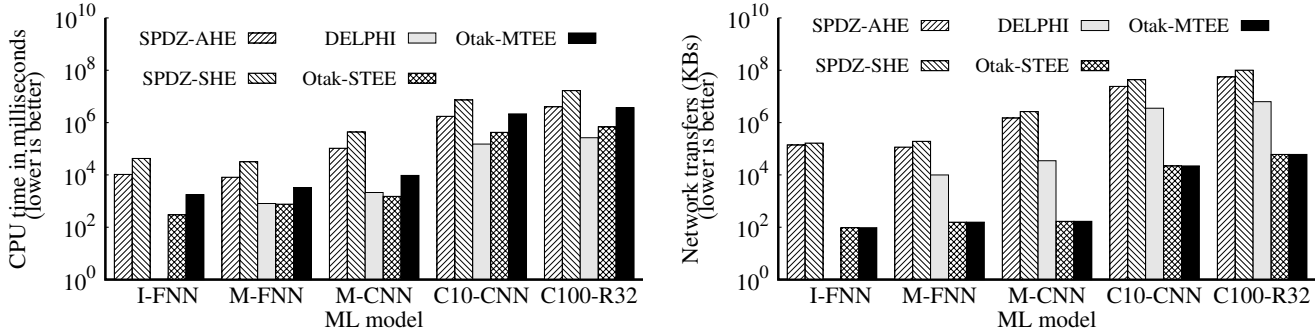


FIGURE 13—CPU time and (wide-area) network transfers for Otak and baseline systems for various ML models. DELPHI does not support Tanh for ISOLET-FNN (I-FNN). Otak’s CPU times are higher than prior work’s CPU time. However, Otak reduces the expensive network transfers. SecureML (not shown in the figure) currently only implements the ReLU function, and can, therefore, encode just the MNIST-FNN (M-FNN) model. For this model, its CPU and network overhead is $9.8\times$ and $46.4\times$, respectively, higher than Otak-MTEE’s.

	I-FNN	M-FNN	M-CNN	C10-CNN	C100-R32
SecureML	-	\$0.48	-	-	-
SPDZ-AHE	\$12.15	\$10.26	\$130.82	\$2129.13	\$4918.67
SPDZ-SHE	\$11.56	\$17.75	\$242.38	\$4044.48	\$9337.42
DELPHI	-	\$0.48	\$1.67	\$169.73	\$301.71
Otak-STEE	$\zeta 0.84$	\$0.02	\$0.03	\$5.63	\$10.68
Otak-MTEE	\$0.03	\$0.05	\$0.15	\$31.43	\$55.94

FIGURE 14—Dollar costs for 1000 private predictions. Otak’s dollar costs are lower as it reduces wide-area network transfers substantially.

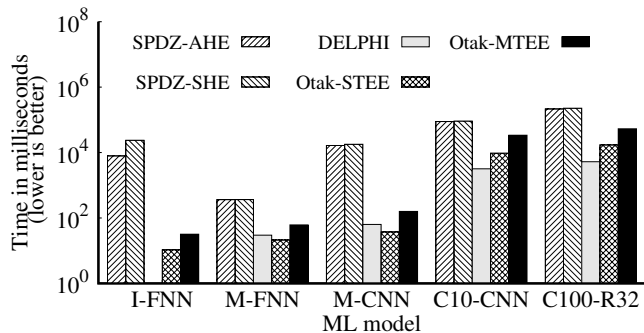


FIGURE 15—Inference latency for Otak and baseline systems. DELPHI does not support Tanh for I-FNN. Otak’s difference to DELPHI is fundamental—DELPHI targets a non-outsourced setting where model parameters are in plaintext while Otak hides the model parameters from the service provider. This difference in setting enables DELPHI to have a very efficient online phase [80].

from the provider. Owing to the difference in setting, DELPHI’s operations are cheaper than Otak’s in its online phase.

Client-side costs for the data point owner are small. For instance, for the largest model (C100-R32), the data point owner expends 2 ms in CPU time and 61.2 KB in network transfers to send secret shares of input image and receive the output label.

Accuracy. We compare Otak’s inference accuracy against TensorFlow’s for I-FNN, M-FNN, M-CNN, C10-CNN, and C100-R32. Otak outputs the correct label 97.5%, 97.6%, 97.2%, 81.6%, and 68.3% of the time, while TensorFlow outputs cor-

rect label 99.0%, 97.8%, 98.3%, 82.7%, and 69.8% of times. Otak’s accuracy is 1-2% lower than TensorFlow’s because it approximates floating-point as fixed-point numbers while TensorFlow does not require such approximation (§3).

7.5 Trusted computing base (TCB)

Otak improves over cryptography-based solutions by using TEEs. However, a downside is the trust on TEEs, which Otak mitigates by keeping the size of the functionality inside the TEE small and distributing trust over heterogeneous TEEs. Here, we report the size of the functionality Otak runs inside its TEEs in terms of source lines of code and compare it to the lines of code inside TEEs for prior TEE-based systems.

Otak’s code inside its TEEs is 1,300 lines. This TCB is $14.6\times$ and $29.2\times$ lower than the TCB sizes of PRIVADO and TF trusted, which have 19K and 38K source lines of code inside the TEE [25, 99]. (For PRIVADO we report TCB size from their paper; for TF Trusted [25], we count only the *included* header files in the TEE code as opposed to the entire codebase of library dependencies [50, 98].)

8 Conclusion

Outsourced private ML inference over two servers is an important problem and has attracted considerable attention. Prior systems for this problem employ two-party secure computation (2PC) protocols that incur high overhead. This paper asked the question, can we accelerate 2PC for this setting by employing trusted-hardware in a limited capacity, and found the results to be encouraging. In particular, one can accelerate 2PC by one to two orders of magnitude (§7), by building on recent primitives such as function and homomorphic secret sharing (§3–§5)—while restricting trusted-hardware to a small computation during preprocessing, and without trusting the hardware of a particular vendor. By demonstrating these promising results, this paper opens up new avenues—not just for two-server outsourced ML inference but also for private ML inference in other settings such as three servers.

A MaxPool and Argmax

As mentioned earlier (§3), efficient FSS constructions [17, 19, 20] currently exist only for two functions: a point function and an interval function. These functions can encode a spline function [20], which in turn can encode ReLU, and close approximations of Sigmoid and Tanh [8]. However, a spline cannot directly encode the MaxPool and Argmax functions. Here, we describe how Otak encodes MaxPool and Argmax using a composition of the point and interval functions.

A.1 Maxpool

Note that max over an array of inputs can be expressed using multiple instances of max over two inputs using a tournament-like tree structure. So we focus on encoding the latter.

Problem with a straightforward encoding. A straightforward approach to expressing the max of two elements $x, y \in \mathbb{Z}$ is to use the sign function:

$$\text{sign}(x - y) = \begin{cases} 1 \text{ (+ve)}, & \text{if } z \geq 0; \\ 0 \text{ (-ve)}, & \text{otherwise.} \end{cases}$$

If the sign of $x - y$ is 1, then the max equals x , else the max equals y . However, as noted earlier (§3), the reasoning above does not work when operating over elements of \mathbb{Z}_p (instead of elements of \mathbb{Z}) as \mathbb{Z}_p is not an ordered ring (when encoding both positive and negative integers).

Otak's encoding of max. Observe that $\text{sign}(x - y)$ gives the right answer when both x and y have the same sign, that is, when they are either both positive or both negative. For this case, we can write $\max(x, y) = \text{ReLU}(x - y) + y$. For the case when x and y have different signs, we can write $\max(x, y) = \text{ReLU}(x) + \text{ReLU}(y)$. Therefore, Otak expresses max as

$$\max(x, y) = \begin{cases} \text{ReLU}(x - y) + y, & \text{if } \text{sign}(x) = \text{sign}(y); \\ \text{ReLU}(x) + \text{ReLU}(y), & \text{otherwise.} \end{cases}$$

To combine the two cases, define a function $b(x, y)$ as

$$b(x, y) = \begin{cases} 1, & \text{if } \text{sign}(x) = \text{sign}(y); \\ 0, & \text{otherwise.} \end{cases}$$

Then,

$$\begin{aligned} \max(x, y) &= b(x, y) \cdot (\text{ReLU}(x - y) + y) \\ &\quad + (1 - b(x, y)) \cdot (\text{ReLU}(x) + \text{ReLU}(y)). \end{aligned}$$

Let $pf_\alpha^\beta(\cdot)$ denote the point function that outputs β at the point α and zero otherwise. Then, given the value of $\text{ReLU}(x) + \text{ReLU}(y)$, one can see that $pf_0^1(\text{ReLU}(x) + \text{ReLU}(y))$ equals 1 if both x and y are negative and zero otherwise. Similarly, $pf_0^1(\text{ReLU}(x) + \text{ReLU}(y) - x - y)$ equals 1 if both x and y are positive and zero otherwise. Hence, $b(x, y)$ can be defined as

$$\begin{aligned} b(x, y) &= pf_0^1(\text{ReLU}(x) + \text{ReLU}(y)) \\ &\quad + pf_0^1(\text{ReLU}(x) + \text{ReLU}(y) - x - y). \end{aligned}$$

With the above definition of the function $b(\cdot, \cdot)$, Otak can express max using point and interval functions. Note that Otak evaluates max over two rounds. In the first round, it computes the shares of the inner parts of the functions (that is, $\text{ReLU}(x - y) + y$ and $\text{ReLU}(x) + \text{ReLU}(y)$), while in the second round, it computes the outer parts of the functions.

A.2 Argmax

Like for Maxpool, Otak's goal is to express Argmax in terms of point and interval functions.

Recall that the Argmax function outputs the index of the maximum entry in an array. Let the inputs to argmax be x_i for $i \in [1, n]$ and let μ equal the biggest value, that is, $\mu = \max(\{x_i\})$, computed using MaxPool (Appendix A.1). Then, one can express the output of argmax as an array of n entries, with 0 at the i -th entry if $x_i \neq \mu$, and the index i at the i -th entry if $x_i = \mu$.

Let $pf_\alpha^\beta(\cdot)$ denote the point function that outputs β at the point α and zero otherwise. Then, we define i -th entry of the Argmax's output as $pf_0^i(x_i - \mu)$, where $\mu = \max(\{x_i\})$.

B Security of the distributing-trust step

Lemma B.1. *Let $G: X \rightarrow Y$ be a PRG. Define $G': X \times X \times X \rightarrow Y$ as $G'(x_1, x_2, x_3) = G(x_1) \oplus G(x_2) \oplus G(x_3)$. Then, the following holds: for every $i, j \in \{1, 2, 3\}$ and $i \neq j$,*

$$\{(G'(x_1, x_2, x_3), x_i, x_j)\}_{x_1, x_2, x_3 \xleftarrow{s} X} \approx_c \{(u, x_i, x_j)\}_{\substack{x_i, x_j \xleftarrow{s} X \\ u \xleftarrow{s} \mathcal{U}}}$$

(\approx_c denotes computational indistinguishability).

In other words, G' is a PRG and moreover, is secure even if any two blocks of the seed of the PRG is revealed to a distinguisher.

Proof. It suffices to prove the case when $i = 2, j = 3$ and the other cases follow symmetrically. From the security of G , which says that an output of G is indistinguishable from an element sampled uniformly at random, the following holds:

$$\begin{aligned} \{(G(x_1) \oplus G(x_2) \oplus G(x_3), x_2, x_3)\}_{x_1, x_2, x_3 \xleftarrow{s} X} \\ \approx_c \{(u \oplus G(x_2) \oplus G(x_3), x_2, x_3)\}_{\substack{x_2, x_3 \xleftarrow{s} X \\ u \xleftarrow{s} \mathcal{U}}} \end{aligned}$$

Since XOR-ing the uniform distribution with any fixed value still gives the same distribution, we have the following:

$$\{(u \oplus G(x_2) \oplus G(x_3), x_2, x_3)\}_{\substack{x_2, x_3 \xleftarrow{s} X \\ u \xleftarrow{s} \mathcal{U}}} \equiv \{(u, x_2, x_3)\}_{\substack{x_2, x_3 \xleftarrow{s} X \\ u \xleftarrow{s} \mathcal{U}}}$$

(\equiv denotes perfect indistinguishability). Combining the above two observations, we have the proof of the lemma. \square

Theorem B.1. *Let $\mathcal{F}_{gen}: (1^\lambda, b, \widehat{f}_r) \mapsto k_b$ for $b \in \{0, 1\}$ denote the functionality (from §5) that outputs BGI keys to M_b . For any PPT adversary \mathcal{A} corrupting $M_b, T_b^{(i)}$ for $i \in \{0, 1, 2\}$, with access to TEEs $T_b^{(j)}, T_b^{(k)}$, for $j, k \in \{0, 1, 2\}$ and $j \neq$*

$i, k \neq i$, for every large enough security parameter λ , there exists a PPT simulator Sim such that the following holds:

For every $b \in \{0, 1\}$, randomness $r_b \in \{0, 1\}^{\text{poly}(\lambda)}$

$$\text{View}_{\mathcal{A}}^{\mathcal{F}_b^{(j)}, \mathcal{F}_b^{(k)}}(1^\lambda, b; r) \approx_{c, \epsilon} \text{Sim}(1^\lambda, b, r, k_b)$$

Remark. The proof essentially follows from Lemma B.1 and the simulation security of the ABY³ protocol in the honest-majority setting.

C Security Proof

We first present the proof for the single-TEE case and later, we show how to extend this proof to the multiple-TEE setting.

C.1 Single-TEE

Suppose there exists a PPT adversary \mathcal{A} that compromises the general purpose machine M_b and TEE machine T_b for some $b \in \{0, 1\}$. We then construct a PPT simulator Sim as follows.

1. Sim chooses a uniform random tape for M_b, T_b .
2. **In setup phase:**
 - (a) Sim simulates the Diffie-Hellman protocol.
 - (b) Sim runs the corresponding simulator of Yao's protocol (see [71] for its description) such that the simulated circuit outputs the simulated share (pk, e_b) , of the HSS keys, to machine M_b .
3. **In model-loading phase:** for every layer in the model,
 - (a) Sim runs the corresponding simulator of Yao's protocol [71]; the simulated garbled circuit is programmed to output an element in R_q^2 , chosen uniformly at random, to machine M_b .
 - (b) Sim picks a matrix in $\mathbb{Z}_p^{m \times n}$, uniformly at random, for layer parameters, and sends it to machine M_b .
4. **In preprocessing phase:** for every layer in the model,
 - (a) Simulator Sim gets the public key pk from the simulated setup phase. For every $i \in \{1, \dots, m\}$, it sends encryption of 0 to M_b .
 - (b) Sim computes the simulator of the BGI protocol, on input $(1^\lambda, b)$, to obtain the simulated key k_b . The functionality inside T_b will now output the key k_b .
5. **In online phase:**
 - (a) Simulator Sim sends shares sh_b^0 , chosen uniformly at random, to machine M_b .
 - (b) For every layer of the ML model, Sim computes the simulator of the secure Beaver multiplication.
 - (c) At the end of every execution of the FSS protocol (one per non-linear layer), the simulator sends a share, chosen uniformly at random, to M_b .

We show that the real world distributions is computationally indistinguishable to the simulated distributions via the standard hybrid argument.

1. Hyb_0 : This corresponds to the real world distribution where the model-owner, the datapoint-owner, secure hardware machine T_b , and general-purpose machine M_{1-b}

execute the system as mentioned in the description of the protocol.

2. Hyb_1 : In this hybrid, the simulator for the Diffie-Hellman key exchange is executed. $\text{Hyb}_0 \approx_c \text{Hyb}_1$ follows from the simulation security of the DH key exchange.
3. Hyb_2 : In this hybrid, we call the simulator of Yao's protocol on input 1^λ and the circuit $\text{Cir}_{\text{setup}}$ that outputs honestly generated BKS-LPR keys: $pk, e_b \in_R R_q^2$. $\text{Hyb}_1 \approx_c \text{Hyb}_2$ follows from the simulation security of Yao's protocol.
4. Hyb_3 : In this hybrid, we modify $\text{Cir}_{\text{setup}}$ such that it outputs simulated BKS-LPR keys: $pk, e_b \in_R R_q^2$ to machine M_b . $\text{Hyb}_2 \approx_c \text{Hyb}_3$ follows from the fact that honestly generated BKS-LPR key is indistinguishable from the simulated key.
5. Hyb_4 : In this hybrid, we again call the simulator of Yao's protocol Sim_{Yao} on input $sh_b^{\mathbf{B}[i]}$ and the circuit $\text{Cir}_{\text{transform}}$ that outputs additive secret shares $sh_b^{\mathbf{B}[i] \cdot s} \in R_q^2$ for each i -th column $\in \{1, \dots, m\}$ to machine M_b . $\text{Hyb}_3 \approx_c \text{Hyb}_4$ due to the simulation security of Yao's protocol.
6. Hyb_5 : In this hybrid, we modify $\text{Cir}_{\text{transform}}$ such that it outputs a value in R_q^2 , chosen uniformly at random, for each i -th column $\in \{1, \dots, m\}$ to machine M_b . Hyb_4 is identical to Hyb_5 due to the perfect security of the secret shares.
7. Hyb_6 : In this hybrid, we change the inputs sent by the model-owner and the machine M_{1-b} to the general-purpose machine M_b . Instead of sending secret shares of the model parameters \mathbf{Y} , model-owner sends a value in $\mathbb{Z}_p^{n \times m}$, chosen uniformly at random. Similarly, instead of sending secret shares $sh_{b-1}^{(\mathbf{Y}-\mathbf{B})}$, machine M_{b-1} sends a value in $\mathbb{Z}_p^{m \times n}$, chosen uniformly at random. Hyb_5 is identical to Hyb_6 due to the perfect security of additive secret sharing scheme.
8. $\text{Hyb}_{7.(j)}$ for j^{th} layer: In this hybrid, we change the ciphertext sent by the machine M_{b-1} to machine M_b in the execution of the j^{th} layer. Specifically, instead of sending encryption of sh_{b-1}^a , machine M_{b-1} sends encryption of $\mathbf{0} \in \mathbb{Z}_p^{1 \times n}$.
The following holds from the semantic security of the LPR scheme: (i) for $j \in \{1, \dots, L-1\}$, where L is the number of layers, $\text{Hyb}_{7.(j)} \approx_c \text{Hyb}_{7.(j+1)}$ and, (iii) $\text{Hyb}_6 \approx_c \text{Hyb}_{7.(1)}$.
9. Hyb_8 : In this hybrid, we invoke the simulator of BGI protocol to obtained simulated key k_b that is then sent to M_b . $\text{Hyb}_8 \approx_c \text{Hyb}_{7.(L)}$ due to the security of the BGI protocol.
10. Hyb_9 : This corresponds to the output distribution of Sim . Hybrids Hyb_8 and Hyb_9 are identically distributed.

C.2 Multiple-TEE

We now focus on the setting when there are multiple TEEs.

Suppose there exists a PPT adversary \mathcal{A} that compromises the general purpose machine M_b and TEE machine $T_b^{(i)}$ for

some $b \in \{0, 1\}, i \in \{0, 1, 2\}$. Let j, k be such that $j \neq i$ and $j \neq k$. We then construct a PPT simulator Sim as follows.

1. Sim chooses a uniform random tape for $M_b, T_b^{(i)}$. Sim simulates the other TEEs T_b^j, T_b^k , where $i \neq j \wedge i \neq k$.
2. **In setup phase:** execute the setup phase of the simulator described in the single-TEE setting.
3. **In model-loading phase:** execute the model-loading phase of the simulator in the single-TEE setting.
4. **In preprocessing phase:** for every layer in the ML model,
 - (a) Same as the Single-TEE case.
 - (b) Sim runs the simulator of Theorem B.1 and outputs simulated BGI key k_b to the machine M_b .
5. **In online phase:** execute the online phase of the simulator described in the single-TEE setting.

We show that the real world distributions is computationally indistinguishable to the simulated distributions via the standard hybrid argument.

1. Hyb_0 : This corresponds to the real world distribution where the model-owner, the datapoint-owner, secure hardware machine T_b^j, T_b^k , and general-purpose machine M_{1-b} execute the system as mentioned in the description of the protocol.
2. $Hyb_{1,(i,1)}$: In this hybrid, the \mathcal{F}_{gen} functionality for generating the BGI keys for the i^{th} layer is simulated using the simulator of \mathcal{F}_{gen} from Theorem B.1. The simulator of \mathcal{F}_{gen} receives as input the BGI key k_b for the i^{th} layer.
3. $Hyb_{0,(i,2)}$: In this hybrid, the simulator for the i^{th} layer \mathcal{F}_{gen} protocol receives as input k_b , where k_b is generated by computing the simulator of the BGI scheme. $Hyb_{0,(i,1)} \approx_c Hyb_{0,(i,2)}$ follows from the security of the BGI scheme. $Hyb_{0,(i,2)} \approx_c Hyb_{0,(i+1,1)}$, for $i < L$ where L is the number of the layers in the ML model, follows from the simulation security of the \mathcal{F}_{gen} protocol.
4. Hybrids Hyb_1 to Hyb_8 are the same as described in the single-TEE setting. $Hyb_{0,(L,2)} \approx_c Hyb_1$ follows from the simulation security of the DH key exchange.

D Workloads

M-FNN consists of 3 dense (that is, fully-connected) layers with ReLU activations for each layer [68, 83]. I-FNN is composed of two dense layers and uses Tanh activations [94]. M-CNN consists of one convolution layer with 5x5 filters, one average pooling layer with 2x2 pool size, and two dense layers that use ReLU activations [72]. C10-CNN uses seven convolutional layers with 3x3 and 1x1 filters, two average pooling layers with 2x2 pool size, and one fully-connected output layer [72, 80]. Finally, C100-R32 uses 32 convolutional layers with 3x3 filters, 30 ReLU activation layers, several add layers (used by shortcut paths), one global average pooling layer, and one fully-connected output layer [80]. We omit stride and padding sizes of convolution layers here and refer

the reader to prior work for their details.

E Pricing model

For network transfers, we directly use the prices reported by the cloud providers for inbound, outbound, and local data transfers. To get the hourly CPU cost, we take the hourly machine cost and split it into CPU cost and memory cost by making a simplifying assumption that two-third of the total machine cost is due to CPU and one-third is due to memory. In reality, pricing resources is an involved task that also depends on factors such as business demand [5, 7]. Therefore, our derived resource prices should only be treated as estimates.

Network pricing. Azure and AWS both do not charge for inbound traffic or local network transfers. For outbound traffic, both these providers charge at \$0.5 per GB [6, 78].

CPU pricing. The hourly prices of m5.4xlarge, D16s-v3, L8s-v2, and DC1s-v2 when reserved for three years are \$0.337, \$0.406, \$0.264, and \$0.119, respectively [7, 79]. Combining this data with the specifications of these machines (that is, the number of CPUs and amount of RAM), and the method described above, we get the following per hour CPU cost: \$0.015 for m5.4xlarge, \$0.017 for D16s-v3, \$0.022 for L8s-v2, and \$0.079 for the SGX-enabled DC1s-v2.

Acknowledgments

We thank Ishtiyaque Ahmad, Alvin Glova, Rakshith Gopalakrishna, Arpit Gupta, Abhishek Jain, Srinath Setty, Jinjin Shao, Tim Sherwood, Michael Walfish, and Rich Wolski for feedback and comments that improved this draft.

References

- [1] O. Abdel-Hamid, A.-r. Mohamed, H. Jiang, L. Deng, G. Penn, and D. Yu. Convolutional neural networks for speech recognition. *IEEE/ACM Transactions on audio, speech, and language processing*, 22(10):1533–1545, 2014.
- [2] M. Albrecht, M. Chase, H. Chen, J. Ding, S. Goldwasser, S. Gorbunov, S. Halevi, J. Hoffstein, K. Laine, K. Lauter, S. Lokam, D. Micciancio, D. Moody, T. Morrison, A. Sahai, and V. Vaikuntanathan. Homomorphic encryption security standard. Technical report, HomomorphicEncryption.org, November 2018.
- [3] Amazon. Law enforcement information requests. <https://www.amazon.com/gp/help/customer/display.html?nodeId=GYSDRGWQ2C2CRYEF>.
- [4] Amazon. Machine learning on AWS-Amazon Web Services. <https://aws.amazon.com/machine-learning/>.
- [5] Amazon Web Services. Amazon Sagemaker Pricing. <https://aws.amazon.com/sagemaker/pricing/>.
- [6] Amazon Web Services. Network Pricing. <https://aws.amazon.com/ec2/pricing/on-demand/>.
- [7] Amazon Web Services. Reserved Instance Pricing. <https://aws.amazon.com/ec2/pricing/reserved-instances/pricing/>.
- [8] H. Amin, K. M. Curtis, and B. R. Hayes-Gill. Piecewise linear approximation applied to nonlinear function of a neural network. *IEE Proceedings-Circuits, Devices and Systems*, 144(6):313–317, 1997.
- [9] W. Arthur and D. Challenger. *A Practical Guide to TPM 2.0: Using the Trusted Platform Module in the New Age of Security*. Apress, 2015.
- [10] A. A. Badawi, J. Chao, J. Lin, C. F. Mun, S. J. Jie, B. H. M. Tan, X. Nan, K. M. M. Aung, and V. R. Chandrasekhar. The AlexNet moment for homomorphic encryption: HCNN, the first homomorphic CNN on encrypted data with GPUs. *arXiv preprint 1811.00778*, 2018.

- [11] M. Ball, B. Carmer, T. Malkin, M. Rosulek, and N. Schimanski. Garbled neural networks are practical. Cryptology ePrint Archive, Report 338.
- [12] R. Barry and D. Volz. Ghosts in the Clouds: Inside China’s Major Corporate Hack. *The Wall Street Journal*, Dec. 2019. <https://www.wsj.com/articles/ghosts-in-the-clouds-inside-chinas-major-corporate-hack-11577729061>.
- [13] D. Beaver. Efficient multiparty protocols using circuit randomization. In *CRYPTO*, 1991.
- [14] F. Boemer, Y. Lao, and C. Wierzynski. nGraph-HE: A graph compiler for deep learning on homomorphically encrypted data. *arXiv preprint 1810.10121*, 2018.
- [15] B. Bond, C. Hawblitzel, M. Kapritsos, K. R. M. Leino, J. R. Lorch, B. Parno, A. Rane, S. Setty, and L. Thompson. Vale: Verifying high-performance cryptographic assembly code. In *USENIX Security*, 2017.
- [16] F. Bourse, M. Minelli, M. Minihold, and P. Paillier. Fast homomorphic evaluation of deep discretized neural networks. In *CRYPTO*, 2018.
- [17] E. Boyle, N. Gilboa, and Y. Ishai. Function secret sharing. In *EUROCRYPT*, 2015.
- [18] E. Boyle, N. Gilboa, and Y. Ishai. Breaking the circuit size barrier for secure computation under DDH. In *CRYPTO*, 2016.
- [19] E. Boyle, N. Gilboa, and Y. Ishai. Function secret sharing: Improvements and extensions. In *ACM CCS*, 2016.
- [20] E. Boyle, N. Gilboa, and Y. Ishai. Secure computation with preprocessing via function secret sharing. In *TCC*, 2019.
- [21] E. Boyle, N. Gilboa, Y. Ishai, H. Lin, and S. Tessaro. Foundations of homomorphic secret sharing. In *Innovations in Theoretical Computer Science Conference (ITCS)*, 2018.
- [22] E. Boyle, L. Kohl, and P. Scholl. Homomorphic secret sharing from lattices without FHE. In *EUROCRYPT*, 2019.
- [23] F. Brasser, U. Müller, A. Dmitrienko, K. Kostianen, S. Capkun, and A.-R. Sadeghi. Software grand exposure: SGX cache attacks are practical. In *USENIX Workshop on Offensive Technologies*, 2017.
- [24] A. Brutzkus, O. Elisha, and R. Gilad-Bachrach. Low latency privacy preserving inference. In *Int. Conference on Machine Learning*, 2019.
- [25] Cape Privacy (formerly Dropout Labs). TF-trusted allows you to run TensorFlow models in secure enclaves. <https://github.com/capeprivacy/tf-trusted>.
- [26] H. Chabanne, A. de Wargny, J. Milgram, C. Morel, and E. Prouff. Privacy-preserving classification on deep neural network. Cryptology ePrint Archive, Report 35, 2017.
- [27] V. Chen, V. Pastro, and M. Raykova. Secure computation for machine learning with SPDZ. In *NIPS*, 2018.
- [28] C. Chevalier, P.-A. Fouque, D. Pointcheval, and S. Zimmer. Optimal randomness extraction from a Diffie-Hellman element. In *EUROCRYPT*, 2009.
- [29] E. Chou, J. Beal, D. Levy, S. Yeung, A. Haque, and L. Fei-Fei. Faster CryptoNets: Leveraging sparsity for real-world encrypted inference. *arXiv preprint 1811.09953*, 2018.
- [30] C. Cimpanu. Cisco removed its seventh backdoor account this year, and that’s a good thing. *ZDNet Zero Day*, Nov. 2018. <https://www.zdnet.com/article/cisco-removed-its-seventh-backdoor-account-this-year-and-thats-a-good-thing/>.
- [31] G. Corfield. Vengeful sacked IT bod destroyed ex-employer’s AWS cloud accounts. Now he’ll spent rest of 2019 in the clink. *The Register*, Mar. 2019. https://www.theregister.co.uk/2019/03/20/steffan_needham_aws_rampage_prison_sentence_voova/.
- [32] V. Costan and S. Devadas. Intel SGX explained. Cryptology ePrint Archive, Report 86, 2016.
- [33] I. Damgård, V. Pastro, N. Smart, and S. Zakarias. Multiparty computation from somewhat homomorphic encryption. In *CRYPTO*, 2012.
- [34] W. Diffie and M. Hellman. New directions in cryptography. *IEEE transactions on Information Theory*, 22(6):644–654, 1976.
- [35] D. Dua and C. Graff. ISOLET datasets. <http://archive.ics.uci.edu/ml/datasets/ISOLET>, 2017.
- [36] T. Espiner. FBI fears hardware backdoors in US military kit. *ZDNet*, May 2008. <https://www.zdnet.com/article/fbi-fears-hardware-backdoors-in-us-military-kit/>.
- [37] N. Fazio, R. Gennaro, T. Jafarikhah, and W. E. Skeith. Homomorphic secret sharing from Paillier encryption. In *International Conference on Provable Security*, 2017.
- [38] A. Fischer, B. Fuhry, F. Kerschbaum, and E. Bodden. Computation on encrypted data using dataflow authentication. *PETS*, 2020(1):5–25, 2020.
- [39] W. Gayde. Rogue system admin shuts down servers and deletes core files on the day he is fired, now faces up to 10 years in prison. *Techspot*, Mar. 2017. <https://www.techspot.com/news/68753-rogue-system-administrator-shuts-down-servers-deletes-core.html>.
- [40] D. Genkin, L. Pachmanov, I. Pipman, and E. Tromer. Stealing keys from PCs using a radio: Cheap electromagnetic attacks on windowed exponentiation. In *Conference on cryptographic hardware and embedded systems (CHES)*, 2015.
- [41] D. Genkin, I. Pipman, and E. Tromer. Get your hands off my laptop: Physical side-channel key-extraction attacks on PCs. *Journal of Cryptographic Engineering*, 5(2):95–112, 2015.
- [42] R. Gilad-Bachrach, N. Dowlin, K. Laine, K. Lauter, M. Naehrig, and J. Wernsing. CryptoNets: Applying neural networks to encrypted data with high throughput and accuracy. In *Int. Conference on Machine Learning*, 2016.
- [43] O. Goldreich, S. Micali, and A. Wigderson. How to play any mental game. In *ACM STOC*, 1987.
- [44] I. Goodfellow, Y. Bengio, and A. Courville. *Deep learning*. MIT press, 2016.
- [45] Google. Asylo: An open and flexible framework for enclave applications. <https://github.com/google/asylo>.
- [46] Google. Government requests for cloud customer data. <https://cloud.google.com/security/transparency/govt-requests>.
- [47] Google Cloud. Method: projects.predict | AI Platform Prediction. <https://cloud.google.com/ai-platform/prediction/docs/reference/rest/v1/projects/predict>.
- [48] Google Cloud. Network Pricing. <https://cloud.google.com/compute/network-pricing>.
- [49] J. Götzfried, M. Eckert, S. Schinzel, and T. Müller. Cache attacks on Intel SGX. In *European Workshop on Systems Security*, 2017.
- [50] gRPC Authors. gRPC: A high performance, open source universal rpc framework. <https://grpc.io/>.
- [51] S. Haykin. *Neural networks: a comprehensive foundation*. Prentice Hall PTR, 1994.
- [52] K. He, X. Zhang, S. Ren, and J. Sun. Deep residual learning for image recognition. In *Conference on computer vision and pattern recognition*, 2016.
- [53] E. Hesamifard, H. Takabi, and M. Ghasemi. CryptoDL: Deep neural networks over encrypted data. *arXiv preprint 1711.05189*, 2017.
- [54] T. Hunt, C. Song, R. Shokri, V. Shmatikov, and E. Witchel. Chiron: Privacy-preserving machine learning as a service. *arXiv preprint 1803.05961*, 2018.
- [55] T. Hunt, Z. Zhu, Y. Xu, S. Peter, and E. Witchel. Ryoan: A distributed sandbox for untrusted computation on secret data. In *OSDI*, 2016.
- [56] N. Hynes, R. Cheng, and D. Song. Efficient deep learning on multi-source private data. *arXiv preprint 1807.06689*, 2018.
- [57] IBM. CEX7S / 4769 Overview - IBM Systems cryptographic hardware products. <https://www.ibm.com/security/cryptocards/pciicc4/overview>.
- [58] IBM. CryptoCards - HSMS, IBM Systems cryptographic HSMS. <https://www.ibm.com/security/cryptocards/hsms>.
- [59] J. Jia, A. Salem, M. Backes, Y. Zhang, and N. Z. Gong. Memguard: Defending against black-box membership inference attacks via adversarial examples. In *ACM CCS*, 2019.
- [60] X. Jiang, M. Kim, K. Lauter, and Y. Song. Secure outsourced matrix computation and application to neural networks. In *ACM CCS*, 2018.
- [61] M. Juuti, S. Szyller, S. Marchal, and N. Asokan. Prada: protecting against dnn model stealing attacks. In *EuroS&P*, 2019.

- [62] C. Juvekar, V. Vaikuntanathan, and A. Chandrakasan. GAZELLE: A low latency framework for secure neural network inference. In *USENIX Security*, 2018.
- [63] M. Keller, E. Orsini, and P. Scholl. MASCOT: faster malicious arithmetic secure computation with oblivious transfer. In *ACM CCS*, 2016.
- [64] M. Keller, V. Pastro, and D. Rotaru. Overdrive: making SPDZ great again. In *EUROCRYPT*, 2018.
- [65] P. Kocher, J. Jaffe, and B. Jun. Differential power analysis. In *CRYPTO*, 1999.
- [66] A. Krizhevsky, V. Nair, and G. Hinton. CIFAR-10 and CIFAR-100 datasets. <https://www.cs.toronto.edu/~kriz/cifar.html>, 2014.
- [67] A. Krizhevsky, I. Sutskever, and G. E. Hinton. Imagenet classification with deep convolutional neural networks. In *NIPS*, 2012.
- [68] N. Kumar, M. Rathee, N. Chandran, D. Gupta, A. Rastogi, and R. Sharma. Cryptflow: Secure tensorflow inference. In *IEEE S&P*, 2020.
- [69] Y. LeCun, C. Cortes, and C. Burges. MNIST handwritten digit database. <http://yann.lecun.com/exdb/mnist>, 2010.
- [70] S. Lee, M.-W. Shih, P. Gera, T. Kim, H. Kim, and M. Peinado. Inferring fine-grained control flow inside SGX enclaves with branch shadowing. In *USENIX Security*, 2017.
- [71] Y. Lindell and B. Pinkas. A proof of security of Yao's protocol for two-party computation. *Journal of Cryptology*, 22(2):161–188, 2008.
- [72] J. Liu, M. Juuti, Y. Lu, and N. Asokan. Oblivious neural network predictions via MiniONN transformations. In *ACM CCS*, 2017.
- [73] Q. Lou, B. Feng, G. C. Fox, and L. Jiang. Glyph: Fast and accurately training deep neural networks on encrypted data. *arXiv preprint 1911.07101*, 2019.
- [74] V. Lyubashevsky, C. Peikert, and O. Regev. On ideal lattices and learning with errors over rings. In *EUROCRYPT*, 2010.
- [75] T. Meyer. No warrant, no problem: How the government can get your digital data. *ProPublica*, June 2014. <https://www.propublica.org/special/no-warrant-no-problem-how-the-government-can-still-get-your-digital-data/>.
- [76] Microsoft. Government access to data. <https://news.microsoft.com/cloudforgood/policy/briefing-papers/trusted-cloud/government-access-data.html>.
- [77] Microsoft Azure. Azure Machine Learning. <https://azure.microsoft.com/en-us/services/machine-learning/>.
- [78] Microsoft Azure. Pricing - Bandwidth. <https://azure.microsoft.com/en-us/pricing/details/bandwidth/>.
- [79] Microsoft Azure. Pricing - Linux Virtual Machines. <https://azure.microsoft.com/en-us/pricing/details/virtual-machines/linux/>.
- [80] P. Mishra, R. Lehmkuhl, A. Srinivasan, W. Zheng, and R. A. Popa. DELPHI: A cryptographic inference service for neural networks. In *USENIX Security*, 2020.
- [81] A. Moghimi, G. Irazoqui, and T. Eisenbarth. CacheZoom: How SGX amplifies the power of cache attacks. In *Conference on Cryptographic Hardware and Embedded Systems (CHES)*, 2017.
- [82] P. Mohassel and P. Rindal. ABY³: A mixed protocol framework for machine learning. In *ACM CCS*, 2018.
- [83] P. Mohassel and Y. Zhang. SecureML: A system for scalable privacy-preserving machine learning. In *IEEE S&P*, 2017.
- [84] K. G. Narra, Z. Lin, Y. Wang, K. Balasubramaniam, and M. Annavaram. Privacy-preserving inference in machine learning services using trusted execution environments. *arXiv preprint 1912.03485*, 2019.
- [85] O. Ohrimenko, F. Schuster, C. Fournet, A. Mehta, S. Nowozin, K. Vaswani, and M. Costa. Oblivious multi-party machine learning on trusted processors. In *USENIX Security*, 2016.
- [86] T. Orekondy, B. Schiele, and M. Fritz. Prediction poisoning: Towards defenses against dnn model stealing attacks. In *International Conference on Learning Representations (ICLR)*, 2019.
- [87] P. Paillier. Public-key cryptosystems based on composite degree residuosity classes. In *EUROCRYPT*, 1999.
- [88] Raejeanne Skillern. Intel SGX Data Protections Now Available for Mainstream Cloud Platforms. *Intel IT Peer Network*, Feb. 2019.
- [89] A. Rane, C. Lin, and M. Tiwari. Raccoon: Closing digital side-channels through obfuscated execution. In *USENIX Security*, 2015.
- [90] M. Research. Microsoft SEAL (release 3.3). <https://github.com/Microsoft/SEAL>, 2019.
- [91] M. S. Riaz, M. Samragh, H. Chen, K. Laine, K. E. Lauter, and F. Koushanfar. XONN: XNOR-based oblivious deep neural network inference. In *USENIX Security*, 2019.
- [92] M. S. Riaz, C. Weinert, O. Tkachenko, E. M. Songhori, T. Schneider, and F. Koushanfar. Chameleon: A hybrid secure computation framework for machine learning applications. In *ACM ASIA CCS*, 2018.
- [93] J. Robertson and M. Riley. The Big Hack: How China Used a Tiny Chip to Infiltrate U.S. Companies. *Bloomberg Businessweek*, Oct. 2018. <https://www.bloomberg.com/news/features/2018-10-04/the-big-hack-how-china-used-a-tiny-chip-to-infiltrate-america-s-top-companies>.
- [94] B. D. Rouhani, M. S. Riaz, and F. Koushanfar. DeepSecure: Scalable provably-secure deep learning. In *Annual Design Automation Conference*, 2018.
- [95] T. Ryffel, D. Pointcheval, and F. Bach. ARIANN: Low-Interaction Privacy-Preserving Deep Learning via Function Secret Sharing. In *NIPS*, 2020.
- [96] R. Shokri, M. Stronati, C. Song, and V. Shmatikov. Membership inference attacks against machine learning models. In *IEEE S&P*, 2017.
- [97] D. Svozil, V. Kvasnicka, and J. Pospichal. Introduction to multi-layer feed-forward neural networks. *Chemometrics and intelligent laboratory systems*, 39(1):43–62, 1997.
- [98] Tensorflow. Tensorflow core 2.0. https://www.tensorflow.org/versions/r2.0/api_docs.
- [99] S. Tople, K. Grover, S. Shinde, R. Bhagwan, and R. Ramjee. PRIVADO: Practical and secure DNN inference. *arXiv preprint 1810.00602*, 2018.
- [100] F. Tramer and D. Boneh. Slalom: Fast, verifiable and private execution of neural networks in trusted hardware. In *International Conference on Learning Representations (ICLR)*, 2019.
- [101] F. Tramèr, F. Zhang, A. Juels, M. K. Reiter, and T. Ristenpart. Stealing machine learning models via prediction apis. In *USENIX Security*, 2016.
- [102] J. Valinsky. 7 of the biggest hacks in history. *CNN Business*, July 2019. <https://www.cnn.com/2019/07/30/tech/biggest-hacks-in-history/index.html>.
- [103] J. Van Bulck, M. Minkin, O. Weisse, D. Genkin, B. Kasikci, F. Piessens, M. Silberstein, T. F. Wenisch, Y. Yarom, and R. Strackx. Foreshadow: Extracting the keys to the Intel SGX kingdom with transient out-of-order execution. In *USENIX Security*, 2018.
- [104] S. Wagh, D. Gupta, and N. Chandran. SecureNN: 3-party secure computation for neural network training. In *PETS*, 2019.
- [105] S. Wagh, S. Tople, F. Benhamouda, E. Kushilevitz, P. Mittal, and T. Rabin. FALCON: Honest-majority maliciously secure framework for private deep learning. *arXiv preprint 2004.02229*, 2020.
- [106] J. Wallen. Is the Intel Management Engine a backdoor? *TechRepublic*, July 2016. <https://www.techrepublic.com/article/is-the-intel-management-engine-a-backdoor/>.
- [107] F. Wang. Function Secret Sharing (FSS) Library. <https://github.com/frankw2>.
- [108] Wheeler, David. slccount - count source lines of code (SLOC). <https://linux.die.net/man/1/slccount>.
- [109] P. Xie, M. Bilenko, T. Finley, R. Gilad-Bachrach, K. Lauter, and M. Naehrig. Crypto-nets: Neural networks over encrypted data. *arXiv preprint 1412.6181*, 2014.
- [110] Y. Xu, W. Cui, and M. Peinado. Controlled-channel attacks:

- Deterministic side channels for untrusted operating systems. In *IEEE S&P*, 2015.
- [111] A. C. Yao. Protocols for secure computations. In *FOCS*, 1982.
 - [112] S. Zahur and D. Evans. Obliv-C: A language for extensible data-oblivious computation. Cryptology ePrint Archive, Report 1153, 2015.
 - [113] K. Zetter. Ex-Gogler allegedly spied on user e-mails, chats. *Wired*, Sept. 2010. <https://www.wired.com/2010/09/google-spy/>.